



**CERN**  
CH1211 Geneva 23  
Switzerland



Engineering Department

EDMS NO.

**XXXXXXXX**

REV.

**0.1**

VALIDITY

**DRAFT**

REFERENCE

**XXXX**

Date: 2015-09-01

# CHARM Calibration Report 2014-2015

## ABSTRACT :

The first two commissioning processes of the CHARM facility in the EAST HALL area (B 157) are reported for 2014 and 2015. Comparison between FLUKA simulations and RadMON measurements and an outline for further work and recommendations are then discussed.

DOCUMENT PREPARED BY:

N.Mota / EN-STI

DOCUMENT CHECKED BY:

J.Mekki / EN-STI

DOCUMENT APPROVED BY:



**XXX**

XXXXXXX

## 0.1

**DRAFT**

Page 2 of 75

REV. NO.	DATE	PAGES	DESCRIPTIONS OF THE CHANGES
----------	------	-------	-----------------------------



## TABLE OF CONTENTS

Terminology .....	6
1. SCOPE OF THE DOCUMENT .....	8
2. AIM OF CHARM COMISSIONING PERIODS .....	8
3. FACILITY OVERVIEW .....	8
4. Beam and Mixed Field Measurement .....	11
4.1 BEAM INSTRUMENTATION .....	11
4.2 RadMON - Mixed Radiation Field Measurement .....	14
4.3 CALIBRATION FACTORS .....	20
5. IRRAD SAMPLE IRRADIATION EFFECTS ON CHARM IN 2014 .....	21
6. 2014 RESULTS .....	26
6.1 COPPER no shielding – Cu_OOOO .....	27
6.2 Aluminium Holes – AlH OOOO .....	35
6.3 Measurements on the MONTRAC during 2014 Commissioning Period .....	37
6.4 2014 Commissioning period overview .....	42
7. 2015 RESULTS .....	45
7.1 Impact of Cypress intermediate neutron response on HEHeq simulation .....	45
7.2 Aluminium no shielding – Al_OOOO .....	46
7.3 Copper full shielding – Cu_CIIC .....	50
7.4 Copper no shielding – Cu_OOOO .....	53
7.5 Measurements on the MONTRAC from 18.05.2015 to 29.06.2015 .....	60
7.6 2015 Data summary tables with ratio of Data/FLUKA .....	65
7.7 2015 Commissioning period overview .....	67
8. COMPARISON WITH FLUKA .....	67
9. FUTURE MEASUREMENTS, RECOMMENDATIONS .....	68
9.1 Completing the FLUKA – RadMON benchmark .....	68
9.2 Building on current RadMON data set .....	70
9.3 Working with IRRAD to understand influence on the CHARM mixed radiation field downstream and managing CHARM response accordingly .....	71
10. REFERENCES .....	68
11. Appendixes .....	72
11.1 Online data files .....	72
11.2 Extrapolation of nuclear interaction range of Silicon for 24 GeV/c protons .....	73



## TABLE OF FIGURES

Figure 3-1 Diagram of LHC with Eat hall Area highlighted in red box, served by PS beam .....	9
Figure 3-2 Building map of Meyrin area highlighting East Hall location in Building 157 .....	9
Figure 3-3 Technical drawing of East Hall Area showing CHARM on line T8.....	10
Figure 3-4: CHARM testing chamber. Left: official simulated positions 2014, Montrac on position M. Right: official simulated positions 2015 (can be accessed by automated conveyor), Montrac on position 6. This figure portrays all of the shielding (from top to bottom: concrete, iron, iron concrete) placed into the testing chamber .....	11
Figure 4-1 Diagram of a 3-foil secondary emission chamber.....	12
Figure 4-2 Scheme of MWPC, equipotential field lines and co-ordinate measurement .....	13
Figure 4-3 MWPC output for a Copper target run .....	13
Figure 4-4: The IRRAD Beam Profile Monitor .....	14
Figure 4-5 Left to right: RadMON V4, RadMON V5 and V6 with deported modules. ....	15
Figure 4-6: The normalised dose does not change with time. The initial asymptote is due to the initial difference in magnitude of the POT and Dose units .....	18
Figure 5-1 Layout of T8 beam line for IRRAD and CHARM irradiation chambers .....	21
Figure 5-2 ION and SEC2 register an increase of approximately 20% coinciding exactly with the insertion of samples at IRRAD. SEC1 and PR.DCBEFEJE_2:INTENSITY showing beam intensity of the PS before second ejection show no difference. ....	22
Figure 5-3 Output of a script to detect IRRAD sample insertion times (raw mV/ SEC counts) according to a threshold in change for SEC2 data. Showing event of 22/11/2014.....	23
Figure 5-4 Factors involved in verifying the influence of IRRAD work on the mixed radiation field on the CHARM testing chamber using RadMONs.....	25
Figure 5-5 Stopping power of Silicon for protons peaking at 60KeV (range: 0.66 $\mu$ m) and exemplifying ever smaller interaction with protons at higher energies (maximum of 10 GeV shown) Source: [9].....	25
Figure 6-1: Positions tested in 2014, also scored in FLUKA. M is the in-beam Montrac position. ....	26
Figure 6-2: TID agreement between data and FLUKA for all tested positions in 2014 in the Cu_OOOO configuration. Normalised with 2015 SEC calibration. ....	29
Figure 6-3: $\Phi_{eq}$ agreement between data and FLUKA for all tested positions in 2014 in the Cu_OOOO configuration .....	29
Figure 6-4: HEHeq agreement between data and FLUKA for all tested positions in 2014 in the Cu_OOOO configuration. Note the expanded different y axis ending in 0.6 .....	30
Figure 6-5: Dose measurements on position 4 over the course of 20 days .....	32
Figure 6-6: $\Phi_{eq}$ measurements on position 4 over the course of 20 days.....	32
Figure 6-7: Dose measurements on position 15 over the course of 20 days .....	34
Figure 6-8: $\Phi_{eq}$ measurements on position 15 over the course of 20 days.....	34
Figure 6-9: Alh_OOOO R factor measurement on P3 .....	35
Figure 6-10: Agreement between TID measurement and simulation for AlH_OOOO .....	36
Figure 6-11 Technical drawing of the Montrac. It allows the placement of 5 electronic boards in parallel. It is angled to the left due to the path of the beam (see Figure 5-1).....	37
Figure 7-1 Positions 1 and 2 with V6#7 motherboard at beam height and motherboards V5#3 and V5#5 above and below. DMV6#7 is at the side of MBV6#7. ....	46
Figure 7-2 1 MB V6 with DM6 plus V5DM#3 and V5DM#5 above .....	48
Figure 7-3: Agreement between V6 data and simulation on TID for Al_OOOO .....	48
Figure 7-4: Agreement between V6 data and simulation on HEHeq for Al_OOOO using new factors as described in section 7.5.....	49
Figure 7-5: Agreement between 1-MeV neutron equivalent fluence measurements and simulation on $\Phi_{eq}$ for Al_OOOO.....	49
Figure 7-6: Agreement between V6 data and simulation on HEHeq for Cu_CIIC.....	51



Figure 7-7: Agreement between 1-MeV neutron equivalent measurement and simulation for Cu_CIIC. A data/FLUKA ratio of 0.56 to 0.96 strongly suggests a correlation with position on $\Phi_{eq}$ fluence, with $2.55E11 \Phi_{eq} \text{ cm}^2$ . This needs to be verified in simulation. ....	52
Figure 7-8: Agreement between V6 data and simulation on TID for Cu_OOOO .....	58
Figure 7-9: Agreement between V6 data and simulation on HEHeq for Cu_OOOO .....	59
Figure 7-10: Agreement between V6 data and simulation on $\Phi_{eq}$ for Cu_OOOO .....	59
Figure 7-11 Both RadFET cards and mounted in the Montrac : Left: RadFET(x15) and Right: RadFET (x27) 60	
Figure 7-12 PIN diodes and RadFET cards installed on the Montrac. Profile view of both cards - note that the RadFET card was placed in front .....	60
Figure 9-1: Dose measurement by V5 and V6 on a 5Gy/hr C60 facility .....	70

## TABLE OF TABLES

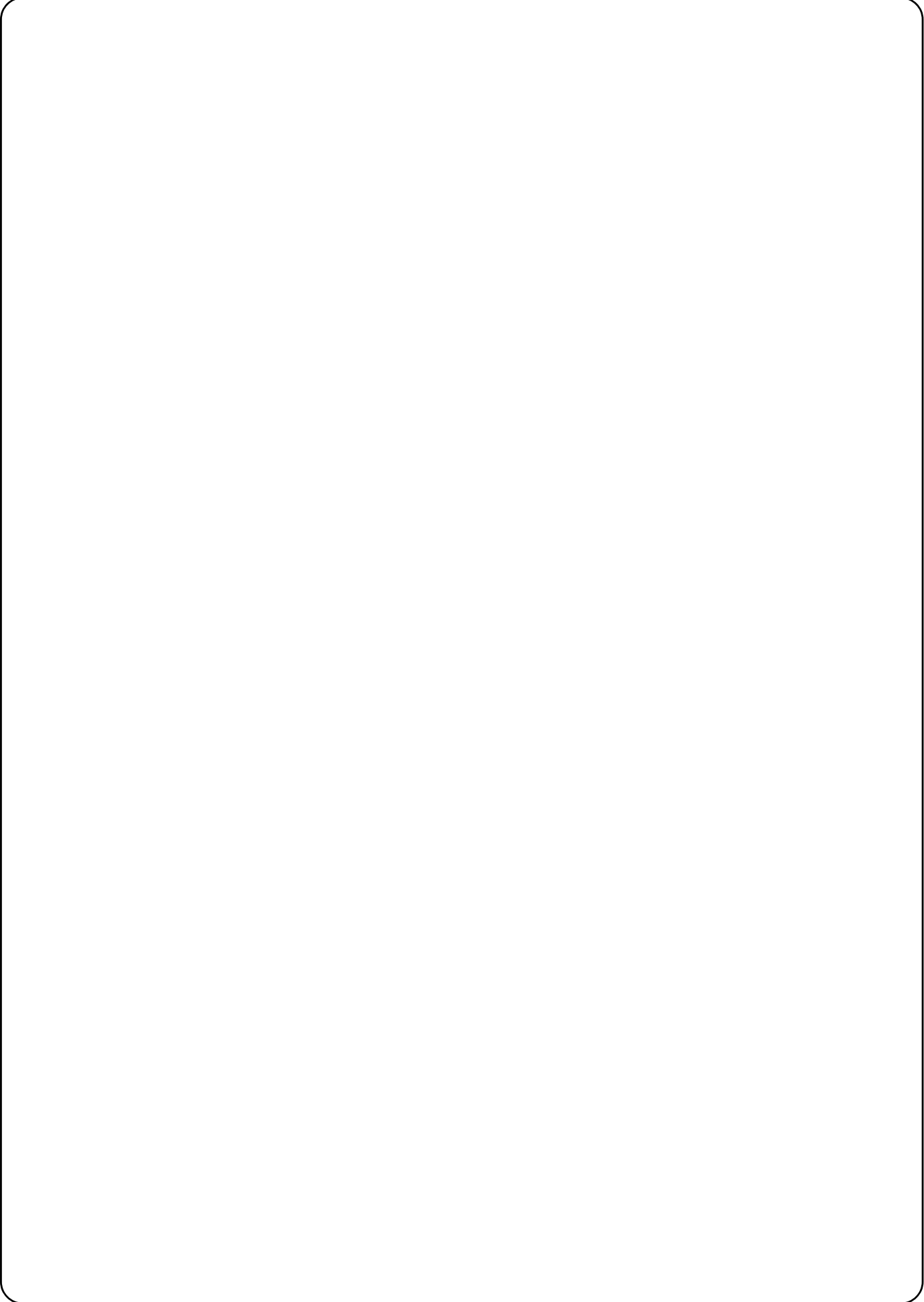
Table 1: RadMON configuration for 2014 and 2015 CHARM commissioning periods .....	15
Table 2: RadMON version comparison. Source: (ref S th) .....	16
Table 3: SRAM cross sections.....	19
Table 4: Range of positions measured during the 2014 Commissioning period .....	26
Table 5 Summary of RadMON testing positions 2014. This does only details measurements done at beam height .....	27
Table 6: Range of beam-height measurements during 2014 commissioning period .....	28
Table 7: Repeated measurements for positions 4 and 7.....	31
Table 8: Repeated measurements for positions 11 and 15.....	33
Table 9: Data set for AIH_OOOO measurements with independent RadMON R factor .....	35
Table 10: Small CU_CIIC run with measurements .....	36
Table 11: Montrac measurements during the 2014 commissioning period .....	37
Table 12: Setup of the scan testing on the Montrac for 31 <sup>st</sup> of October .....	38
Table 13: Intensity scan results for deported modules on the 31 October run .....	38
Table 14: Direct beam with no target measurements .....	39
Table 15: Blown up beam configuration measurements.....	39
Table 16: Blown up beam configuration with intensity scan .....	40
Table 17: Montrac measurements using deported modules during 2014 commissioning .....	40
Table 18: Normalised dose factors for short circuit RadFET grid. The grid was installed at the Montrac test location to evaluate the beam profile at this location using the copper target .....	41
Table 19 Summary of 2014 AIH OOOO results .....	42
Table 20 Short CU CIIC run .....	43
Table 21: Montrac averages normalised by POT. FLUKA data available soon. ....	43
Table 22: Summary of 2014 CU OOOO results .....	44
Table 23: Increment factors on simulated HEHeq values from Toshiba to Cypress SRAM.....	45
Table 24: Measurements on Position 1 with V5 and V6.....	46
Table 25: Normalised data for positions 2-7 for the AI_OOOO configuration.....	47
Table 26: Results for AI_OOOO on position 9 using both V5 and V6 .....	47
Table 27: Normalised results for P1 on Cu_CIIC configuration. V5 results not available. ....	50
Table 28: Normalised results for positions 2-9.....	50
Table 29: Measurements done on position 1 for CU_OOOO configuration for V6 RadMONs.....	53
Table 30: Measurements done on position 1 for CU_OOOO configuration for V5 RadMONs.....	54
Table 31: Measurements performed on positions 2-5 in the Cu_OOOO configuration.....	55
Table 32: Results from position 9 on CU_OOOO with RadMON V6.....	56



Table 33: Results from position 9 on CU_OOOO with RadMON V5.....	56
Table 34: Results from position 7, single result from position 10 on Cu_OOOO with RadMON V6 .....	57
Table 35: Montrac irradiation run in the 2015 Commissioning period .....	60
Table 36: Dose measurements on the Montrac with a short circuit RadFET array .....	61
Table 37: Dose measurements on the Montrac with a short circuit RadFET array .....	62
Table 38: 1-MeV Neutron $\Phi_{eq}$ measurements on the Montrac with a PIN diode array .....	63
Table 41: 1-MeV Neutron $\Phi_{eq}$ measurements on the Montrac with a PIN diode array .....	63
Table 40: Dose measurements on the Montrac with a short circuit RadFET array .....	64
Table 42 Summary of 2015 Cu OOOO results.....	65
Table 43 Summary of 2015 Al OOOO results.....	66
Table 44 Summary of 2015 CU CIIC results .....	67
Table 45: Online file repository. This can change in the future. ....	74

## Terminology

**ADC:** Analog to digital converter  
**CCC:** Cern control center  
**DD:** Displacement damage  
**H4IRRAD:** Irradiation facility for LHC equipment, intalled in the H4 beamline (SPS North area)  
**IRRAD:** Proton irradiation facility  
**CHARM:** CERN High energy AcceleRator Mixed Field/Facility  
**PS:** Proton Synchrotron  
**R2E:** Radiation-to-Electronics  
**RADFETS:** Radiation-sensing Field-effect Transistors  
**RadMON:** Radiation Monitoring System  
**SEU:** Single evet upset  
**TID:** Total Ionising Dose  
**THn:** Thermal Neutron  
**HEH:** High energy hadrons  
 **$\Phi_{eq}$ :** 1-MeV neutron equivalent fluence  
**SRAM:** Static Random Access Memory  
**SEC:** Secondary count monitor  
**MWPC:** Multi-wire proportional chamber  
**BuB:** Blown up beam  
**BPM:** Beam positioning Monitor





## 1. SCOPE OF THE DOCUMENT

This document gives a complete summary for the commissioning periods at CHARM from 2014 to 2015. Comparison between FLUKA simulations of the radiation levels and RadMON are presented. Circumstances unique to the start-up of the facility are described and experimental directions taken in accordance with these circumstances are explained. Thus the same conditions can be replicated.

## 2. AIM OF CHARM COMMISSIONING PERIODS

1. Start-up of the facility and troubleshooting before user testing
2. Characterisation of the Mixed Radiation field through RadMON and other dosimetry sensor systems
3. Comparison with FLUKA simulations
4. Testing of dosimetry equipment used by the Radiation to Electronics (R2E) group

## 3. FACILITY OVERVIEW

The **CERN** High energy **AcceleRator** **Mixed** **Field** acts as one of the newest CERN irradiation facilities being exploited by the R2E group. It provides a means to stress test and validate electronic equipment in radiation environments which are representative of their real application. Indeed, the CHARM facility produces a mixed radiation field composed of different particle types over a wide energy range. According to the facility configuration and the selected test position, this radiation field can be adjusted to be representative of high energy accelerator, ground level, atmospheric, and space environments.



## CERN's Accelerator Complex

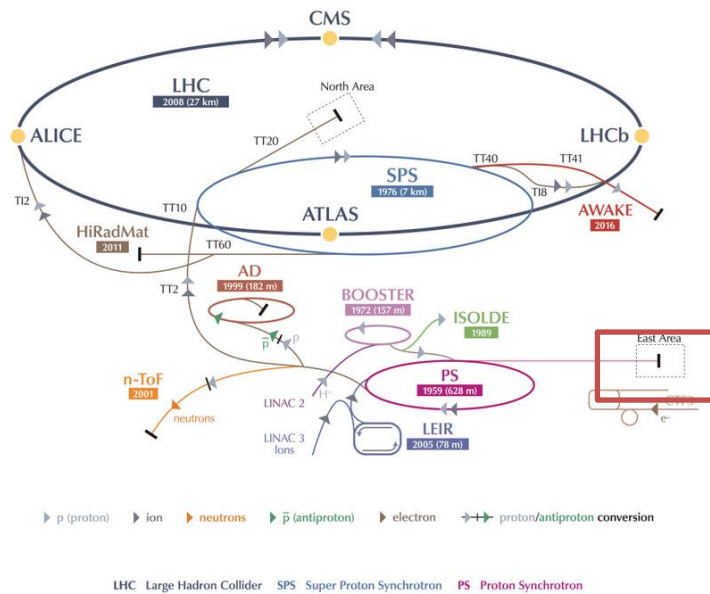


Figure 3-1 Diagram of LHC with East hall Area highlighted in red box, served by PS beam

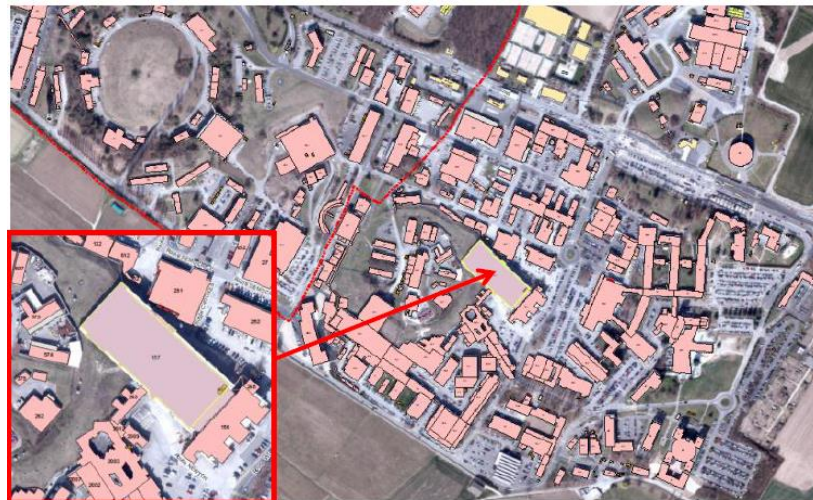


Figure 3-2 Building map of Meyrin area highlighting East Hall location in Building 157

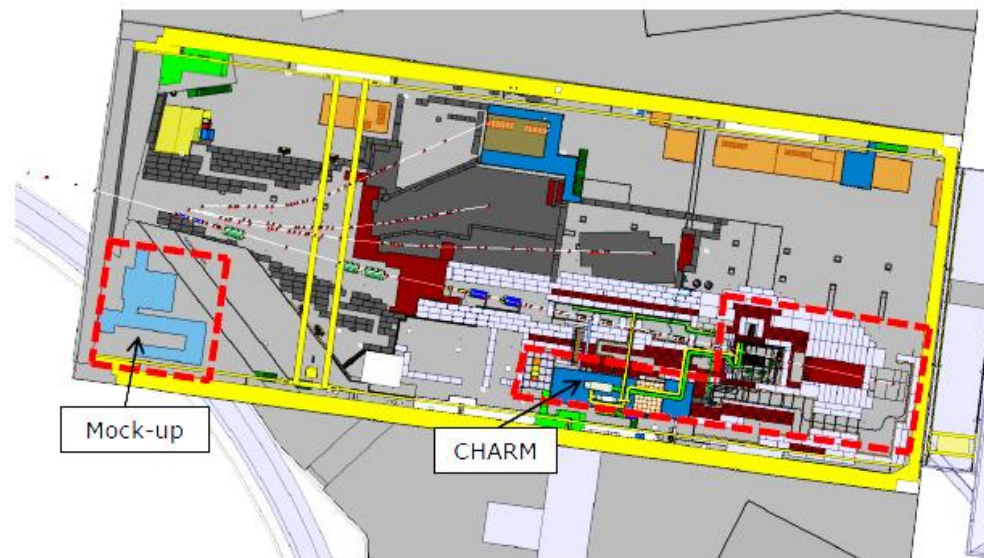


Figure 3-3 Technical drawing of East Hall Area showing CHARM on line T8

The facility hosts metal targets (copper and aluminium) which are placed in a 24 GeV/c proton beam line, extracted from the Proton Synchrotron (T8 beam extraction line).

As the 24 GeV/c proton beam impinges on the target, this induces the production of a mixed radiation field throughout the target chamber (approximately 70 m<sup>3</sup>), where either complete electronics systems and/or hundreds of components can be tested. The profile of this resulting mixed radiation field leads to a range of gradients in the chamber both in intensity and particle spectra.

This can be taken advantage of to reproduce the conditions of the environment on which the electronic components being tested were designed to operate. This is diversified further by using targets of different densities and modular shielding. Therefore, according to the facility configuration, it is possible to match the required radiation environment.

A successful comparison between simulation and measurements (RadMON) is intended to lead to complete characterisation of the radiation levels. This is done by calculating constant radiation field values per position that scale linearly with incoming protons and comparing them to simulation values.

A good characterisation of the radiation levels is needed to provide an accurate dosimetry to the users through on-line measurements of the radiation levels the equipment has been subjected to.

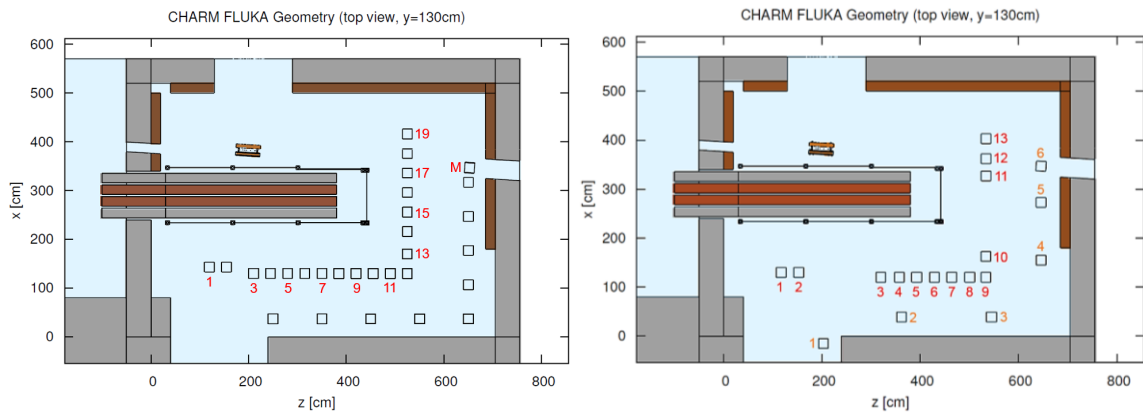


Figure 3-4: CHARM testing chamber. Left: official simulated positions 2014, Montrac on position M. Right: official simulated positions 2015 (can be accessed by automated conveyor), Montrac on position 6. This figure portrays all of the shielding (from top to bottom: concrete, iron, iron concrete) placed into the testing chamber

## 4. Beam and Mixed Field Measurement

### 4.1 BEAM INSTRUMENTATION

The creation of the mixed field at CHARM depends on the profile and the intensity of the beam. Both factors are affected by the stability of the beam although they rarely change from the required value.

At CHARM, the protons on target are measured on a spill-by-spill basis by secondary emission chambers (**SEC**) and the beam profile is measured by a multi-wire proportional chamber (**MWPC**) as well as four beam positioning monitors (**BPM**) located upstream in the IRRAD facility. See chapter 5 for a schematic of the positioning of these monitors.

- **SEC:**

The **S**econdary **E**mission **C**hamber hosts an array of alternatively biased foils at high voltage in hard vacuum. Incoming particles interact with grounded plates, leading to a surface effect where deposited energy liberates surface electrons in the foils. Secondary electrons travel in vacuum to the adjacent anode foil where they are collected and read. A voltage to frequency or current to frequency convertor, depending on the design, is used to calculate the number of charged particles travelling through the SEC.

Importantly, once the SEC counts are correctly calibrated with the particle beam intensity, the number of **POT** that is available to create the mixed field by interacting with the target can be calculated. Calibration runs have been made for SEC1 and SEC2 in 2014 and 2015. more information can be found on [2].

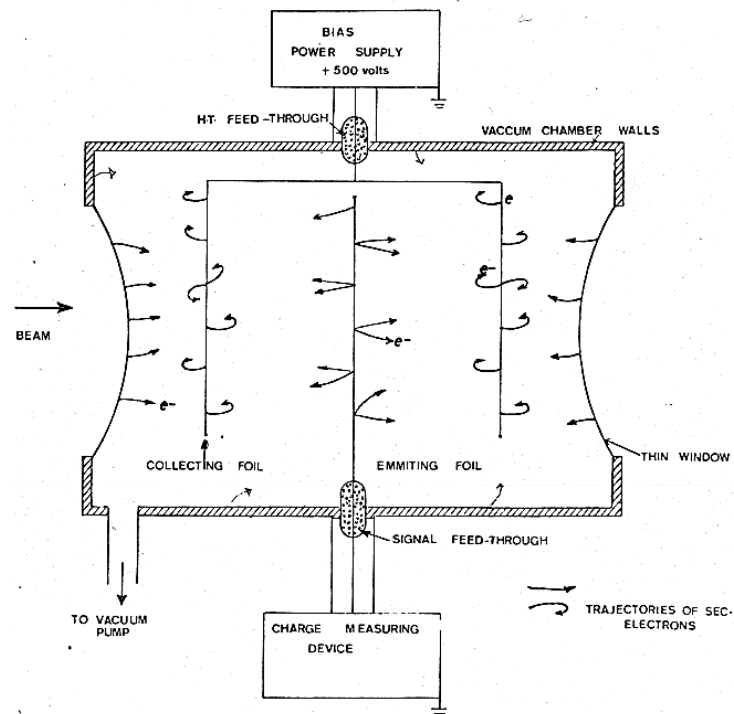


Figure 4-1 Diagram of a 3-foil secondary emission chamber

- **MWPC:**

The multi-wire proportional chamber provides a horizontal and vertical profile view of a particle beam. It is typically found in high energy secondary beam setups. Two tense multi-wire frames for each profile plane are encased in a gas mixture, separated by two cathode grids. Each wire is connected as a channel in the device electronics, leading to spatial information of the beam pulse with basis on gas-filled proportional charge amplification and collection. This method can be used to create devices that can extend for up to square meters of detection area.

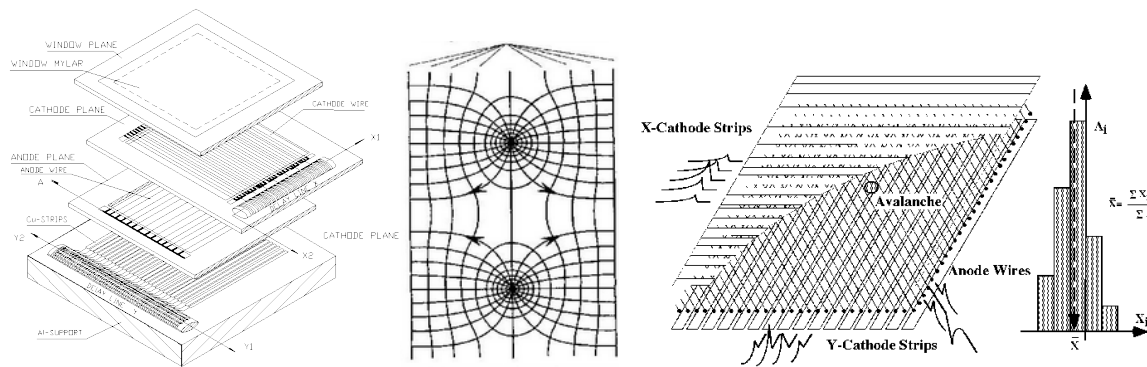


Figure 4-2 Scheme of MWPC, equipotential field lines and co-ordinate measurement

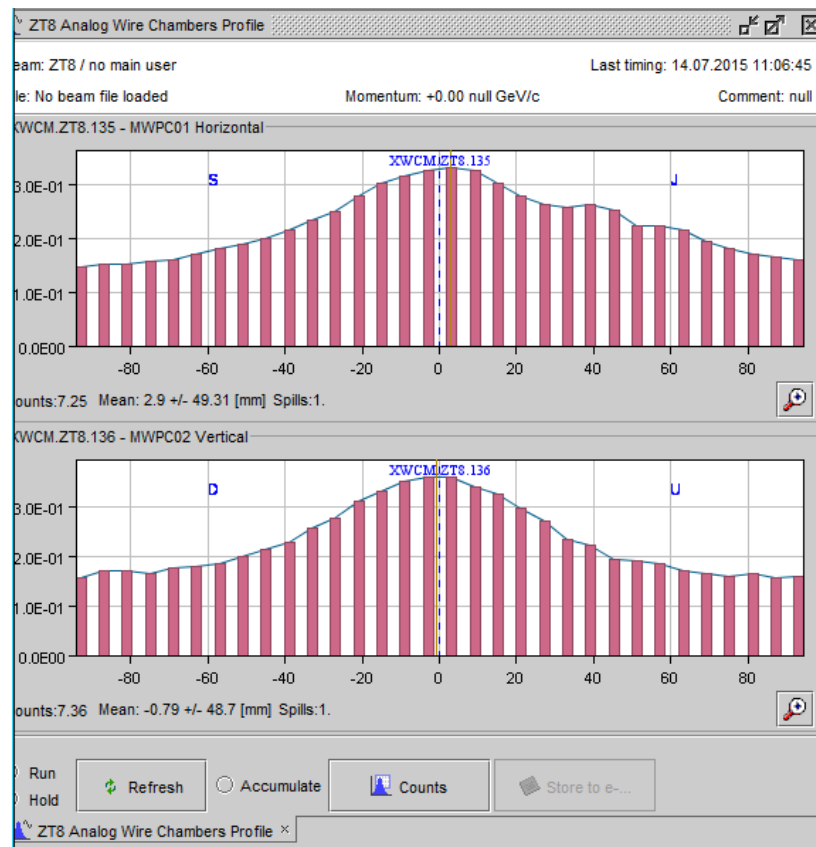


Figure 4-3 MWPC output for a Copper target run

Figure 4-3 shows MWPC output in normal operation when a metal target has been inserted into the beam line. The FWHM of the signal is expanded considerably in this case. The user interface shows the horizontal profile above and vertical profile below for a Cu\_0000 run with an intensity of  $4.5E11$  protons declared by the PS. The x axis is in mm from the center (0 is the center) and the y axis shows an uncalibrated factor proportional to the intensity of the beam.

#### • BPMs:

There are 4 beam profile monitors (BPM) maintained by IRRAD that supplement beam position and profile diagnostics. This instrument bases its operation the emission effect



of secondary electrons. One BPM is located upstream in the same location as SEC 1 and the other three are in one of each of the three irradiation areas of the IRRAD facility.



Figure 4-4: The IRRAD Beam Profile Monitor

## 4.2 RadMON - Mixed Radiation Field Measurement

The RadMON is an integrated dosimetry system [3]. RadMONs are used in CHARM to quantify three main characteristics of the radiation field:

- Total Ionising Dose in Gy= $J/Kg$ ; 1 Gy is equivalent to 100 rad
- High energy hadron fluence  $cm^{-2}$
- 1-Mev neutron equivalent fluence  $cm^{-2}$

The measurements of those parameters are performed by means of RadFETs, SRAM memories and silicon P-I-N diodes respectively, as detailed in the following sections.

The electronic readout of RadFETs, SRAM and PIN diodes is executed by a motherboard processed and sent to a gateway via the WorldFIP<sup>i</sup> bus. The RadMON systems (currently both versions 5 and 6 used at CHARM) also make use of deported modules, allowing these to be placed independently from their motherboards in the test chamber. The deported module contains only PIN diodes and RadFETs, without any readout electronics, allowing measurements in very harsh environments without being damaged by radiation. On the other hand, the motherboard composed by sensors and readout electronics is sensitive to radiation and can survive up to around 80 Gy and 250 Gy for both the RadMON V5 and V6 respectively.

<sup>i</sup> Information on the CERN WorldFIP can be found in [5]



Figure 4-5 Left to right: RadMON V4, RadMON V5 and V6 with deported modules.

#### 4.2.1 Using the RadMON during commissioning periods

As opposed to normal operation periods dedicated to user device irradiation, commissioning periods offer the opportunity to make a range of different measurements with different facility configurations and at different test locations. For instance, measuring HEH and Thermal neutron fluence requires the presence of a motherboard in the testing chamber as both are performed using the SRAM memories embedded on the motherboard, resistant up to 80Gy on V5 and 250Gy on V6.

Commissioning Period	Setup: (Motherboard = MB , Deported Module = DM)	
2014	6 RadMON V5:	4 MB (400nm RadFET) + 4 DM (100nm RadFET)
		2 MB (no RadFET)+ 2 DM (100nm+400nm RadFETs)
2015	6 RadMON V6:	4 MB (400nm RadFET) + 4 DM (100nm RadFET)
		2 MB (no RadFET)+ 2 DM (100nm+400nm RadFETs)
	2 RadMON V5:	2 MB (no RadFET)+ 2 DM (100nm+400nm RadFETs)

Table 1: RadMON configuration for 2014 and 2015 CHARM commissioning periods

The configuration described on Table 1: RadMON configuration for 2014 and 2015 CHARM commissioning periods enables versatility and redundancy in the measurements. There are two radfets allowed per RadMON system. Two deported modules that could be cross checked with this configuration (100nm and 400nm RadFETs) were better suited for measurements in locations with harder radiation and where more detailed TID measurements were needed.

Four motherboards with one embedded 400nm RadFET were better suited for HEH and Thermal neutron measurements as the TID absorbed by the motherboard could be measured directly. The risk in reaching the TID limits of the motherboards could be

carefully managed before and after each irradiation session. Two legacy V5 RadMONs were kept from 2014 to compare measurements with the V6.

	RadMON V5	RadMON V6
ADC	12 bit	16 bit
ADC Resolution	2.4 mV	150μV
100nm GND Resolution [Gy]	1.3	$8.2 \times 10^{-2}$
400nm GND Resolution [Gy]	0.063	$3.93 \times 10^{-3}$
Maximum dose to MB [Gy]	80	250

Table 2: RadMON version comparison. Source: (ref S th)

The sixth version of the RadMON brings considerable improvement over the main drawbacks of the V5. Most importantly, the higher radiation tolerance of 250Gy. It is based on modular architecture enabling efficient maintenance and upgrades. Its configuration can be changed remotely (i.e. SRAM voltage biasing). [3] The 16-bit ADC for sensing has a resolution 16 times higher than the V5 and is pivotal in the large increase in the accuracy of the measurements with comparison to its predecessor and overall device efficiency.

#### 4.2.2 Calibration factors of measurement

Since the beam intensity provided by the PS and the particle momentum does not change, it is reliable to assume that the field intensity per position on the testing chamber should be constant with respect to protons on target, regardless of intensity [1].

This enables the implementation of normalisation factors of the mixed radiation field which are independent through time. This important concept underpins the comparison effort between FLUKA simulations and measurements. Future CHARM research and irradiation planning will only need to rely these calibration factors and allowing to do not use the RadMON motherboard during each run (see 4.2.1, lifetime of the RadMON).

It was decided to improve the reliability of result processing not just by normalising the final dose with the final POT but by normalising these throughout the run. As the radiation flux should be constant for a specific position in a given facility configuration, this normalisation should yield a constant value versus time (or POT). Thus an average of the points past a stabilisation point in the normalisation curve is made as it is shown in Figure 4-6: The normalised dose does not change with time. The initial asymptote is due to the initial difference in magnitude of the POT and Dose units

#### 4.2.3 RadFET:

RadFETs are p-channel MOSFETs. The gate dielectric is thicker than industrial MOSFETs, with the purpose of being sensitive to ionising radiation where electron-hole pairs are created due to deposited energy. Due to the lower mobility of holes, they are trapped in the insulating layer – leading to the storage of information relative to the TID



deposited in the oxide volume. When injecting a constant current through the source, it is found that the threshold voltage  $V_{th}$  at the gate shifts negatively with  $Gy$  as the positive charge from the trapped holes is accumulated through time inside the gate oxide.

The  $\Delta V_{th}$  since the first irradiation of the RadFET is integrated through time, and its non-linear response to ionising radiation dose ( $Gy$ ) is converted to the measured dose with a pre-recorded calibration curve [3]. RadFET's are used in measurement multiple times and since the RadFET response to TID is not linear, the initial voltage of the RadFET must be known. This is used to calculate the TID by shifting the  $\Delta V_0/Gy_0$  of a particular irradiation period starting at  $t_0$  to the correct section of the calibration table.

- Calibration tables

The  $\Delta V_{th}$  shift with respect to dose is retrieved from a lookup table made of the averages of calibration lookup tables made with raw data from RadFET's of the same wafer. The variation in these raw data lookup tables is used to provide a standard deviation with respect to dose. This is embedded in calibration tables made during Fraunhofer measurement campaigns (date?) using Co60 at different dose rates. Uncertainty as the spread between RadFETs from the same batch (wafer) for the  $\Delta V_{th}/Gy$  curve was also embedded in these calibration tables and is attached to every output dose result when operated with a script. [4] demonstrates the superior reliability of the thinnest - 100nm - RadFET under 30-230 MeV range proton beams due to the higher build in field effect, reducing columnar recombination effects at lower energy charged hadrons. Therefore, whenever possible, TID measurements are quoted from 100nm RadFET readings.

- Calculation of the dose:

A Matlab script takes raw data in mV from the RadMON. For the 2015 iteration the data is already formatted from TIMBER<sup>ii</sup> such that it is averaged every 10 seconds for the raw voltage and SEU counts values, and summed every 10 seconds for the SEC values. This was due to the the raw file for V6 dose being too large to be saved in excel (>65000 lines). Then the data could be used in the same way as the legacy Matlab scripts (as opposed to a csv file). This method has been tested against previous methods and other independent calculations [insert reference to Adam's report and Benjamin's tool], with no change in calculated values.

- SEC counts are multiplied by the SEC to POT factor. The factor 2.24E7 is used in the data analysis for this report.
- For script calculations, the POT needs to have the same timing as the cumulative RadFET voltage by interpolation or with method described above (10 second interval)
- Initial voltage of respective RadFET is subtracted from the data set to obtain  $\Delta V_{th}$
- The data set is converted into dose and respective standard deviation error using calibration tables (Matlab function  $V_{th}2Gy3$ )

---

<sup>ii</sup> CERN's sensor database query tool (ref)

- The dose curve over time (integral) is divided by the curve of the sum of protons on target over time.

The dose measured due to stable proton intensity should not change, and this is seen by the stabilisation of the curve of Dose/POT over time (see Figure 4-6). The initially high values in Figure 4-6 are due to the division of very small dose values with very high POT values – the operation is more accurate at the end of the curve. The jaggedness of the curve is due to the resolution of the 100nm RadFET (RadMON V5) dose measurement. This method always yields a normalisation factor slightly lower than the single point normalisation of the final dose with the final POT.

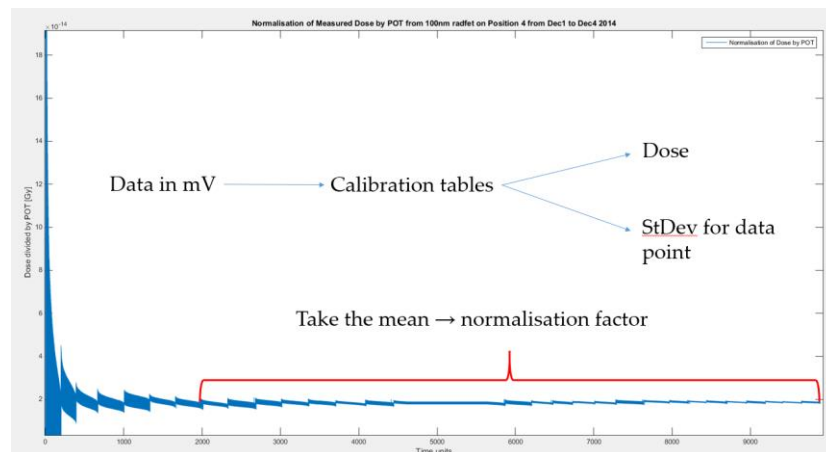


Figure 4-6: The normalised dose does not change with time. The initial asymptote is due to the initial difference in magnitude of the POT and Dose units

Calculation of the normalisation (calibration factor) is done by performing the arithmetic average of the curve past a cutting point where the curve is stable. This cutting point is selected by visual inspection and it is stored in the variable output text file for each run. The cutting point is generally the same for a given set of runs in a commissioning period.

#### RadFETs in short circuit:

As shown in [3] 100nm RadFETs irradiated at 1kGy can lose only up to 3.7% of stored dose via annealing of trapped charges in 100 hours, enabling their suitability in short circuited mode, given that reading is performed usually one week after irradiation. They can be installed on a surrogate RadMON board so that a current can be injected and thus recover TID data. The main difference when the RadFETs are used in short-circuit is that this is a single point measurement only at the end of the irradiation, meaning that the TID is not recorded on-line but the final TID is measured.

#### 4.2.4 SRAM:

The RadMON motherboard is equipped with Static RAM (SRAM) memories [5]. The fluence of high energy hadrons (P,n K, n) can be shown to be correlated with the creation of single event upsets (SEU) in SRAM [5]. SEU is defined reversal of logic gates – *bit flips* – in the memory. There are two main SRAM brands in use: Toshiba and Cypress [2]. The Toshiba memories used on the RadMON are sensitive to thermal

neutrons due to containing B<sup>10</sup> neutron capture reactions [5], whilst Cypress memories have a very small thermal neutron cross section. Both the HEH and thermal neutron fluences are desirable information as their ratio, the Risk factor, or R-factor =  $\Phi_{Th}/\Phi_{HEH}$  is not reliable in simulations.

- Cross sections

The calibration of the Cypress for protons being currently used was measured at PSI in 2011 [3]. The thermal neutron cross section was last verified at REZ [3]. Toshiba memories are qualified in the same way as the Cypress. The latest batch tested at PSI dates in 2014. The batch used for the CHARM RadMONs dates 2012.

	Cross section for Protons	Cross section for Thermal Neutrons
Cypress	$7.48E10^{-13} \pm 8E10^{-14} \text{ cm}^2$	$3.84E10^{-16} \pm 7.5E10^{-17} \text{ cm}^2$
Toshiba 3V	$5.56E10^{-14} \pm 4.86E10^{-15} \text{ cm}^2$	$1.58E10^{-13} \pm 1.02E10^{-13} \text{ cm}^2$
Toshiba 5V	$2.28E10^{-14} \pm 2.89E10^{-15} \text{ cm}^2$	$2.61E10^{-15} \pm 3.04E10^{-15} \text{ cm}^2$

Table 3: SRAM cross sections

- Calculation of HEH, Th neutron fluence, R factor:

Raw integrated SEU counts are acquired from the logging database.

The response does not change with irradiation thus it is not required to keep a record of initial conditions. If both the HEH and the Thermal neutron fluences were calculated in the same position the R factor is readily available and is formulated in this way for the V5:

$$R = \frac{\Phi_{th}}{\Phi_{HEH}} = \frac{\sigma_{HE}^{3V} S_{5V} - \sigma_{HE}^{5V} S_{3V}}{\sigma_{th}^{5V} S_{3V} - \sigma_{th}^{3V} S_{5V}}$$

Equation 4-1 : R factor calculation using V5 RadMON with HEH and Thermal neutron measurement with the Toshiba SRAM memories

Calculating the R factor from two V5 motherboards located at the same position, or when the SRAM voltage that has been changed during 2 runs is available [6] and for one V6 motherboard using both Cypress and Toshiba [3].

The R factor is used in the individual formulas to yield the HEH and thermal neutron fluences. The HEH fluence can be calculated in Toshiba and Cypress memories at 5V and 3.3V respectively and the thermal neutron fluence can be calculated in the Toshiba memories at 3V. For Cypress and Toshiba joint measurements:

$$R = \frac{\sigma_{HEH}^{3V\_Toshiba} S_{Cypress} - \sigma_{HEH}^{Cypress} S_{3V\_Toshiba}}{\sigma_{th}^{Cypress} S_{3V\_Toshiba} - \sigma_{th}^{3V\_Toshiba} S_{Cypress}}$$

Equation 4-2: R factor calculation using Cypress SRAM and Toshiba SRAM biased at 3V

These quantities are normalised with the number of POT to derive their calibration factors as described in 5.3.3.

#### 4.2.5 PIN diodes:

The RadMON system hosts three silicon PIN diodes in series in its deported module. Silicon PIN diodes are measured in forward bias to monitor the increase in the forward voltage  $V_f$  (voltage drop across the diode), which increases as particle radiation interacts and causes displacement damage on the silicon crystal – leading to degradation of conductivity and minority carrier lifetime [7]. This is correlated with 1-MeV neutron equivalent fluence.

- Calibration tables:

Displacement damage tests were made in 2013 on CEA Valdud [5]. Raw data acquired during this test campaign is converted to 1-MeV neutron equivalent fluence using the  $V_f$  to  $\Phi_{eq}$  calibration table made at CEA.

- 1-Mev NEQ Calculation

A script is used to calculate the  $\Phi_{eq}$  in the same fashion as described in 4.2.3. The 1-Mev neutron equivalent fluence is then normalised by the POT as portrayed in Figure 4-6: The normalised dose does not change with time. The initial asymptote is due to the initial difference in magnitude of the POT and Dose units.

### 4.3 CALIBRATION FACTORS

FLUKA simulations report that the field varies linearly with intensity of the primary beam (24 GeV/c protons) to a good approximation [1]. Focusing is done before the target is introduced into the beam, assuring that the whole beam hits the target and contributes to creating the mixed field. Thus the most important variable when analysing the beam input and how it affects measurement is the number of protons hitting the target (Protons On Target: **POT**). This is also true in the case of the blown-up beam configuration (when the beam has been defocused to allow for a larger beam spot at the Montrac test location) where no target is inserted into the beam.

This can be used to obtain the **calibration factors** for the radiation field as a function of test position, using RadMON measurements and/or FLUKA simulations. These are the integral radiation level quantities normalised by the number of POT (i.e. Gy/POT for the TID) which can be applied to any situation in which the POT for the intended irradiation period is known. Ratios of these calibration factors can be used to estimate other

measured radiation field types for the same position where only one other factor is known (i.e. Gy/HEH).

## 5. IRRAD SAMPLE IRRADIATION EFFECTS ON CHARM IN 2014

IRRAD is a facility located directly upstream from CHARM. Both facilities share beam time in the same T8 beamline. IRRAD has three tables in their testing chamber on which samples are placed for irradiation.

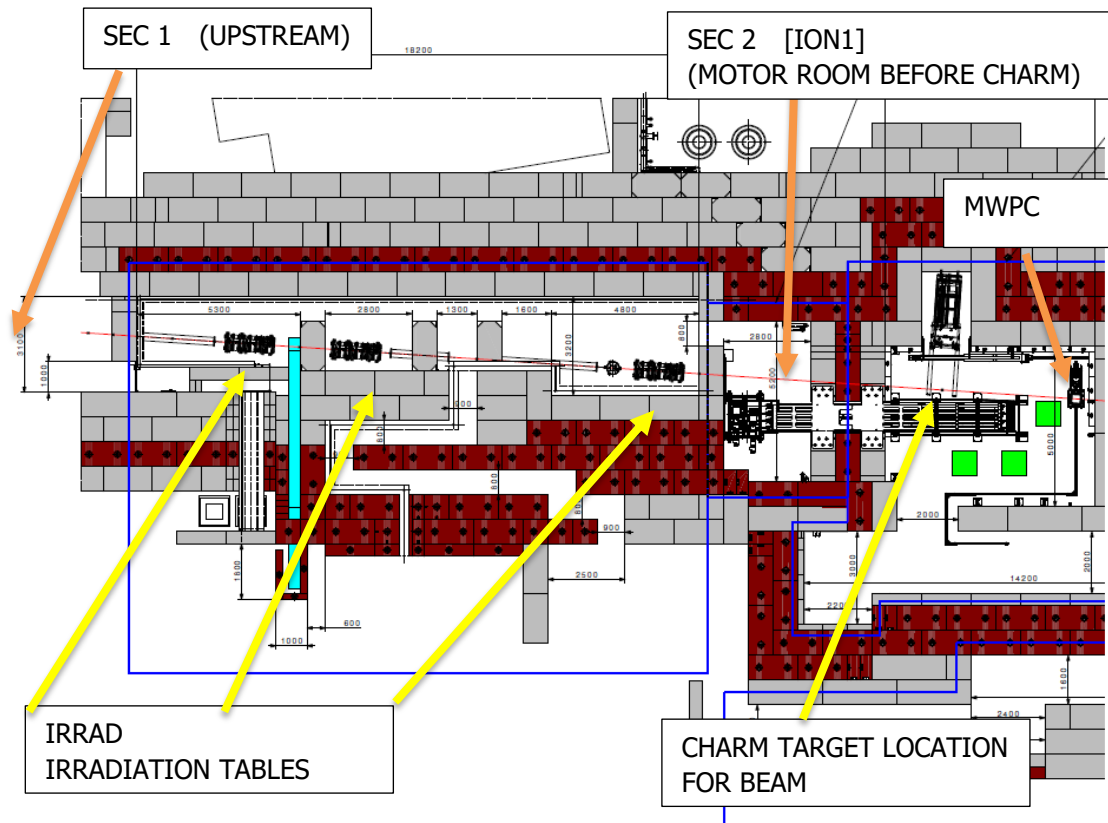


Figure 5-1 Layout of T8 beam line for IRRAD and CHARM irradiation chambers

### 5.1.1 INFLUENCE OF IRRAD ON **POT** MEASUREMENT DOWNSTREAM

During 22 November 2014 it was found that IRRAD sample insertion into the beam coincided with an increase in 15% of counts measured by SEC2 (and ION chamber) downstream at the entrance of CHARM. Output from the PS did not increase and SEC1 did not record any such increase [[e-logbook hyperlink](#)]. Also available on appendix **Error! Reference source not found..**

This behaviour was confirmed on multiple instances of IRRAD sample usage. Due to this fact it was decided to use SEC1 measurements in concordance with its calibration factor (measured as 1.99E7 for 2014 and 2.24E7 for 2015, later in use) to obtain the number of POT.

The first event (Figure 5-2 ION and SEC2 register an increase of approximately 20% coinciding exactly with the insertion of samples at IRRAD. SEC1 and PR.DCBEFEJE\_2:INTENSITY showing beam intensity of the PS before second ejection

show no difference.) was correlated with the insertion of a sample (6cm of LuAG/YAG<sup>iii</sup> crystals) in the IRRAD testing chamber. The samples were such that the interaction of the proton beam with them is thought to have led to an increase of secondary particles being detected downstream due to spallation with the samples.



Figure 5-2 ION and SEC2 register an increase of approximately 20% coinciding exactly with the insertion of samples at IRRAD. SEC1 and PR.DCBEFEJE\_2:INTENSITY showing beam intensity of the PS before second ejection show no difference.

Discussion with IRRAD confirmed that no more than 1cm equivalent of silicon was used in 2014 with the exception of 22.11.2014 and the placement of a cryostat from 05.12.2014 until the end of the 2014 commissioning period (15.12.2015), equivalent to 2mm of silicon and 8 mm of stainless steel.

The effect in SEC2 subsided whenever the samples were removed and this could even be used to indirectly assess the timings of multiple IRRAD samples insertions by seeing 'steps' in the SEC2 counts.

Since the SEC can detect protons, pions and electrons (charge of +1 or -1), given that the incoming particle is fast [8], the general consensus of the matter is that Rutherford scattering and delta rays (electrons) from beam interaction with the samples were propagated downstream, partially aided by vacuum tubes, and lead to this increase on the sec counts.

As a result, it should follow that the increase in the sec counts downstream is characteristic of each IRRAD sample (if enough accuracy could be mustered).

<sup>iii</sup> Lutetium based aluminium garnets (LuAG), Y-based aluminium garnets (YAG), used as scintillator crystals.

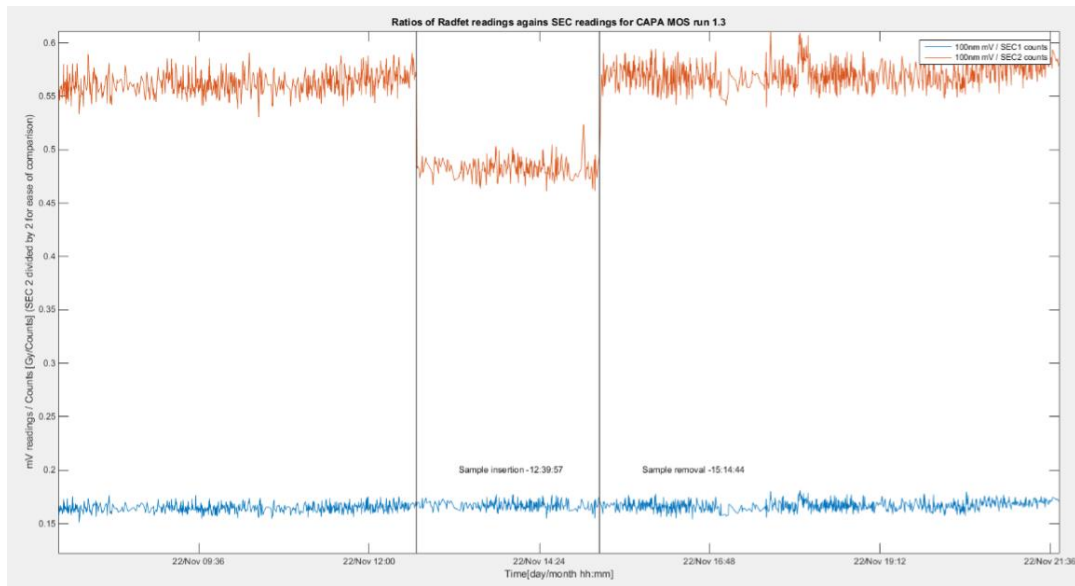


Figure 5-3 Output of a script to detect IRRAD sample insertion times (raw mV/ SEC counts) according to a threshold in change for SEC2 data. Showing event of 22/11/2014.

#### 5.1.2 INFLUENCE OF IRRAD ON CHARM's **MIXED FIELD** DOWNSTREAM IN 2014

It is important to perform comparisons of the radiation levels with an accurate calculation of the number of POT. This could be solved by using the output from SEC1, but this had to be checked against RadMON measurements, together with SEC2 measurements, before, during and after IRRAD sample insertion into the beam.

As seen in the e-logbook the first step was to check directly on Timber using both RadFET raw voltage and SEU counts. Then as shown in Figure 5-3, a ratio of the SEC measurements and the raw data was plotted.

$$\frac{\Delta \text{SEU}_1}{\text{SEC}_1} = \frac{\Delta \text{SEU}_1}{\text{SEC}_2}$$

Equation 5-1: Initial conditions before IRRAD sample insertion into the beam.

The formula above shows the normal operation condition without IRRAD interference. However, if the SEC2 counts increase due to detecting a larger number of charged particles, the fraction will be lower, and this will be seen as a decrease in the ratio. When an IRRAD sample is removed from the beam, initial conditions are regained. SEC1 and SEC2 are different thus their count ratio and respective POT calibration factors are different. This behaviour is what was investigated as shown in Figure 5-3. A raw ratio of the RadFET voltage against the SEC shows in this example that the sample influence on the beam did not affect the RadMON measurement.

In addition, several arguments are available in the support of the proposition that for the scope of the current work on this effect - from 22.11.14 to 15.12.14 – IRRAD sample insertion into the T8 beamline had a negligible effect on the mixed radiation field at

CHARM, given that SEC1 readings are trustworthy and that nothing else has/had an impact in spill intensity and SEC2 measurements:

- Conservation of energy: each beam pulse extracted by the PS loses energy as it travels
  - An increase in counts in SEC2 is due to more charged particles being detected, but the energy of the pulse can only be lower due to attrition with IRRAD samples
  - By definition this should only affect the mixed field at CHARM by lowering the number of available proton momentum or proton count (plus any other particles resultant from previous Rutherford scatterings) that reaches the target – i.e.  $Gy=J/Kg$ .
- FLUKA simulations [1] show that the CHARM mixed field intensity changes linearly with proton intensity at 24 GeV/c – thus why only one factor is simulated per facility configuration in all positions in what concerns incoming beam intensity. Any change of the CHARM mixed field due to IRRAD sample insertion should be in direct relationship with energy lost by these very same insertions
  - In accordance to [9] the stopping power for Silicon for 10 GeV protons (limit of table) was used in retrieving a range (i.e. alpha particles have a range of a few cm in air) of 23.6 meters. A coarse extrapolation resulted in an approximated range of 70m for 24 GeV protons. The Brag peak for protons is close to 60 KeV in Silicon and 150 KeV in Iron (steel in cryostat)
  - This extrapolation suggests that there would be needed the equivalent of 7-8 cm of silicon to reduce the energy of the spill by 1%. Even if possible, this would be too small a fluctuation for the RadMON system [3] .The incoming beam energy would have to be reduced by at least 30% for the RadMON to detect a statistically relevant difference in the mixed field.

Finally, this leads to the solution that only SEC1 counts should be used when calculating the **POT** despite being further away from the CHARM irradiation chamber than SEC2. More information of SEC2 behaviour will be gathered and analysed in the future.



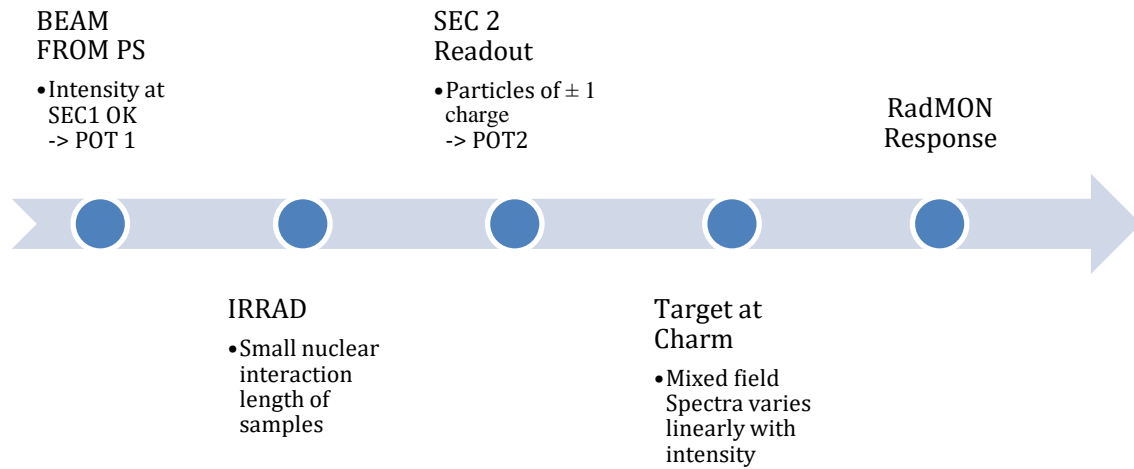


Figure 5-4 Factors involved in verifying the influence of IRRAD work on the mixed radiation field on the CHARM testing chamber using RadMONs

### PSTAR : Stopping Power and Range Tables for Protons

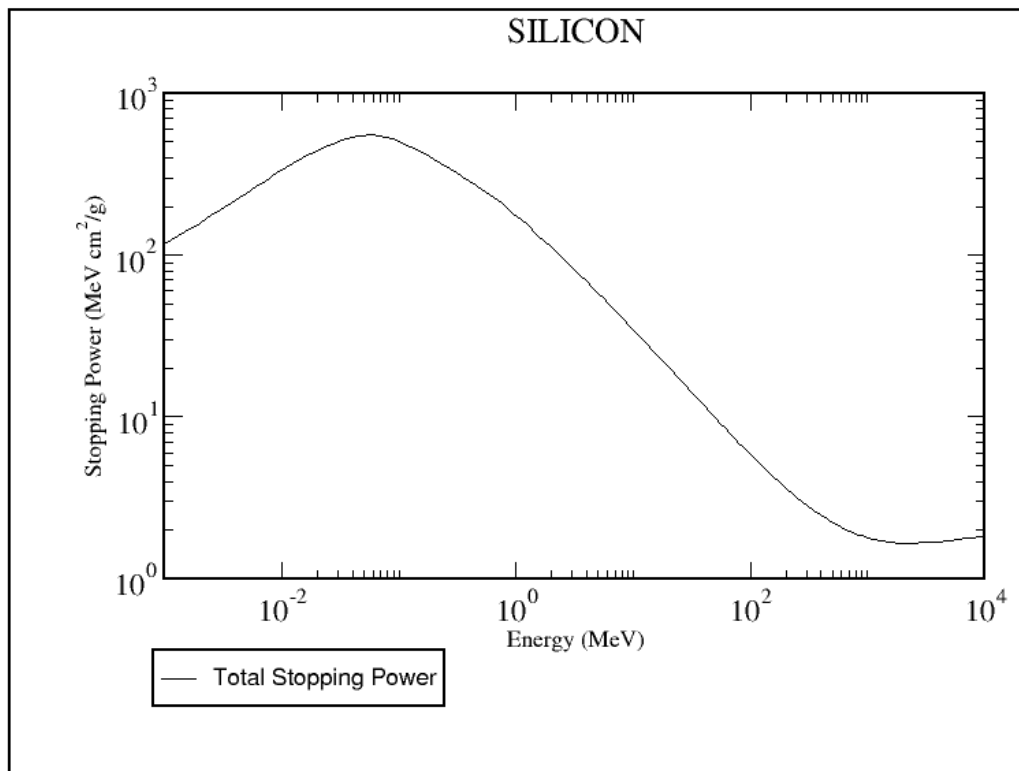


Figure 5-5 Stopping power of Silicon for protons peaking at 60KeV (range: 0.66μm) and exemplifying ever smaller interaction with protons at higher energies (maximum of 10 GeV shown)  
Source: [9]



## 6. 2014 RESULTS

RadMON calibration factors are presented below. These have been categorised by facility configuration and position. The 2014 commissioning period mostly overlapped with user testing, as among other reasons, facility instrumentation and secondary beam settings were being setup for the first time in order to be ready to follow user testing.

From 12/11/14 to 15/12/14 on full irradiation period only four days were used for the BuB<sup>iv</sup> and AIH\_OOOO configurations, and another four for Cu CIIC. The most tested facility configuration was Cu\_OOOO: copper target with no shielding configuration. This was driven by users requesting the highest irradiation settings. This allowed a first comparison between RadMON data and FLUKA for this configuration, predominantly in TID readings.

There was little chance to perform repeat measurements for all positions in 2014. Single measurement errors derived from the RadFET and PIN diode calibration tables are shown from Table 6: Range of beam-height measurements during 2014 commissioning period to Table 10: Small CU\_CIIC run with measurements, whilst a cross section error of 12.7% is appended for HEH results. Whenever these are averaged for a position in the same facility configuration, the highest calibration table error can be quoted.

Data has been recalculated retroactively with 2015 SEC 1 calibration factor of 2.24E7 protons per count.

Facility configuration	TID	HEH & THn Fluence	1-MeV NEQ Fluence
Cu_OOOO	Between P1 & P19	Between P3 & P15	Between P1 & P19
AIH_OOOO	Between P1 & P14	Between P1 & P3	Between P1 & P14
Montrac	Cu & BUB	No Data	Cu

---

<sup>iv</sup> Blown up beam (FWHM of beam profile can be spread to 10cm of diameter)

Table 4: Range of positions measured during the 2014 Commissioning period

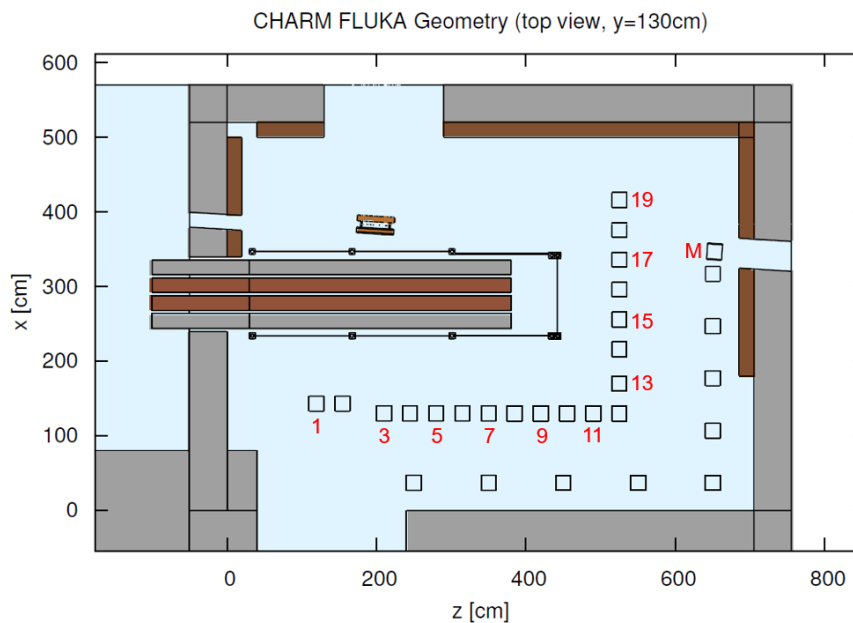


Figure 6-1: Positions tested in 2014, also scored in FLUKA. M is the in-beam Montrac position.

## 6.1 COPPER no shielding –

### Cu\_OOOO

There were 8 Cu\_OOOO runs performed for the 2014 commissioning phase:

Run Start	RadMON V5 positions	Run Start	RadMON V5 positions
Run End		Run End	
12.11.14 16:55	3, 7, 11, 15, 19	01.12.14 13:35	4, 7, 11, 15, M
13.11.14 12:05		04.12.14 08:12	
18.11.14 21:07	3, 14	05.12.14 18:28	4, 7, 11, 15, M
20.11.14 07:00		07.12.14 07:52	
24.11.14 13:16	3, 4, 15	08.12.14 16:12	4, 7, 11, 15, M
27.11.14 13:03		11.12.14 12:36	
28.11.14 12:53	1, 3, 4, 15, 16, F, M <sup>v</sup>	12.12.14 15:36	4, 11, 14, 15, M
30.11.14 15:40		15.12.14 06:00	

Table 5 Summary of RadMON testing positions 2014. This does only details measurements done at beam height

Two main aspects of the 2014 Cu\_OOOO runs were the broad position testing on 12-Nov and the continuous testing on P4 and P15 from 24-Nov to 12-Dec which, importantly, were done at beam height. Thermal neutrons are not compared with FLUKA and were only available as a measurement during a single AIH\_OOOO test.

<sup>v</sup> F: Optical fiber, M: Montrac

The final error on the result is dependent on the standard deviation of the mean calculated as shown in Figure 4-6.

This imposes a minimum TID, HEH, THn and 1-MeV n.e. fluence quantities that must be measured by the RadMON in order to obtain results with acceptable standard deviation error. This creates a competition between TID and HEH measurements, as the RadMON motherboard used to measure the HEH fluence can only survive up to 80 Gy for the RadMON V5. All results are normalised by POT as described in section 4.3.3.

2014 position	POT	Dose [Gy]	HEHeq cm <sup>-2</sup>	1-Mev NEQ cm <sup>-2</sup>
RadMON	Date in	Error %	Error %	Error %
Height from floor	Date out	Data/FLUKA	Data/FLUKA	Data/FLUKA
<b>P1</b>	7.585e+15	7.92E-15		2.17E-04
<b>DM5</b>	24.11.14	4.5%		12.3%
<b>129cm</b>	27.11.14	0.65		0.73
<b>P3</b>	7.0381E+14	2.64E-14	4.39E-05	3.75E-04
<b>DM1</b>	12.11.14	9.4%	12.7%	23.4%
<b>129cm</b>	12.11.14	1.44	0.90	1.15
<b>P7 (P4 New)</b>	7.0381E+14	2.66E-14	5.29E-05	1.81
<b>DM2+MB2</b>	12.11.14	6.5%	12.7%	7%
<b>129cm</b>	12.11.14	1.08	0.96	0.65
<b>P11 (P8 new)</b>	7.0381E+14	2.43E-14	3.83E-05	1.75E-04
<b>DM3</b>	12.11.14	7.6%	12.7%	44%
<b>110cm</b>	13.11.14	1.07	0.81	0.88
<b>14</b>	5.722E+15	1.56E-14		8.61E-05
<b>DM5</b>	12.12.14	3.3%		6.3%
<b>129cm</b>	15.12.14	0.63		0.40
<b>15</b>	7.038E+14	3.30E-14	6.22E-05	1.86E-04
<b>DM5</b>	12.11.14	9.8%	12.7%	42.9%
<b>129cm</b>	12.11.14	0.80	0.73	0.83

<b>16</b>	5.618+15	2.69E-14	1.33E-04
<b>129cm</b>	28.11.14	4.5%	4%
	30.11.14	0.61	0.60
<b>19 (P13 New)</b>	7.0381E+14	3.73E-14	2.15E-04
<b>DM6</b>	12.11.14	5.2%	7.7%
<b>129cm</b>	12.11.14	0.97	0.98

Table 6: Range of beam-height measurements during 2014 commissioning period

All the results in this table show measurements in different positions for the CU\_OOOO configuration. The different times at which they were performed are indicated

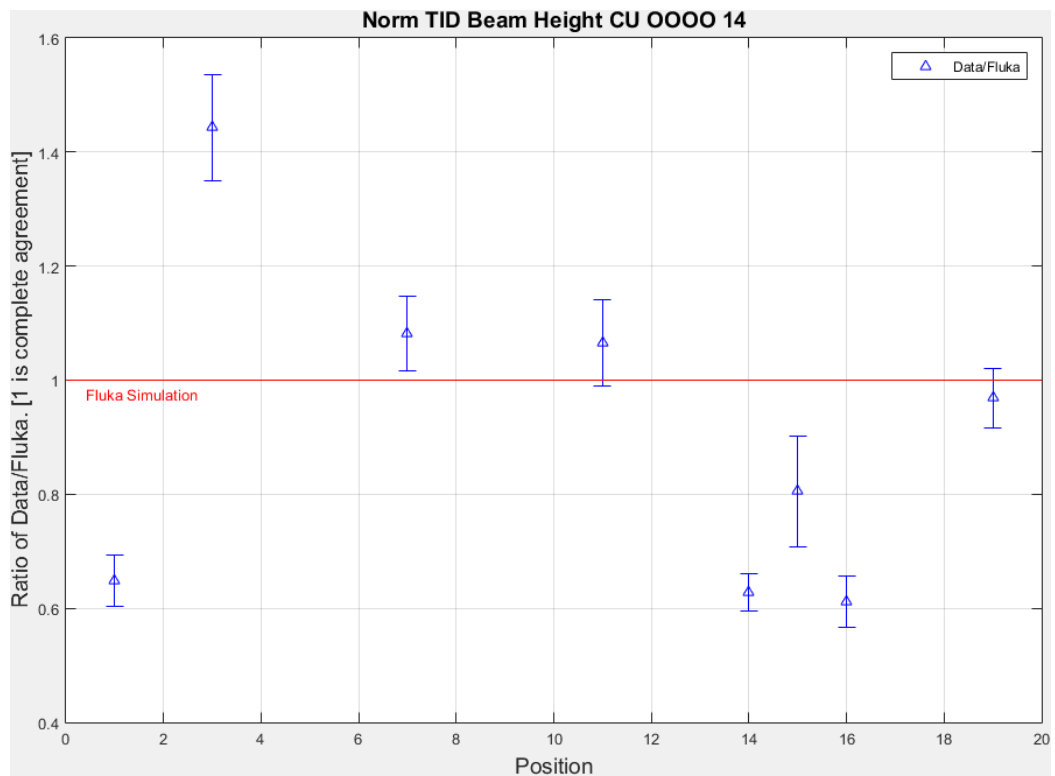


Figure 6-2: TID agreement between data and FLUKA for all tested positions in 2014 in the Cu\_OOOO configuration. Normalised with 2015 SEC calibration.

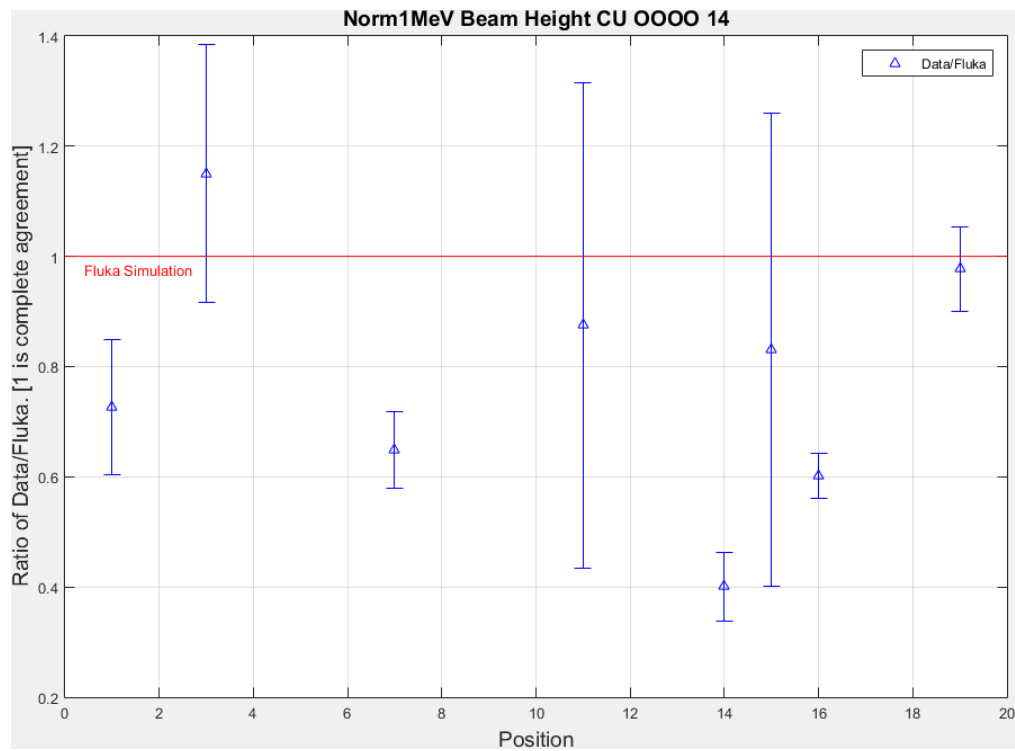


Figure 6-3:  $\Phi_{eq}$  agreement between data and FLUKA for all tested positions in 2014 in the Cu\_OOOO configuration

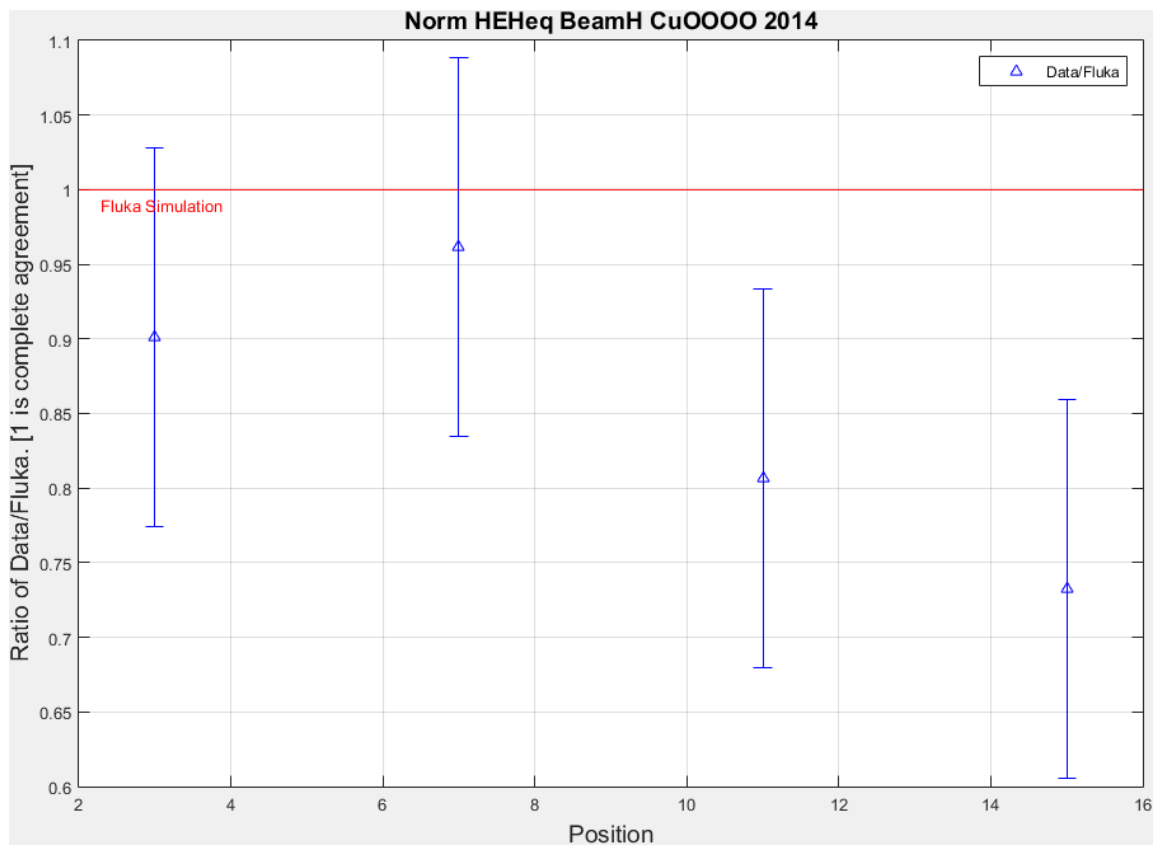


Figure 6-4: HEHeq agreement between data and FLUKA for all tested positions in 2014 in the Cu\_OOOO configuration. Note the expanded different y axis ending in 0.6

The normalised HEH fluence derived from the V5 in 2014 was calculated with a simulated R factor and used as described in 4.2.4. These were then compared to the High Energy Hadron equivalent (HEH<sub>eq</sub>) factor in FLUKA, a quantity taking into account intermediate energy neutrons (below 20 MeV[cm<sup>-2</sup>]) using a Weibull-like fit which is distinct for the RadMON SRAM type being used<sup>vi</sup> [10]:

$$\Phi_{\text{HEH}} = \int_{0.2\text{MeV}}^{20\text{MeV}} \omega(E)\phi_n(E)dE + \int_{20\text{MeV}}^{\infty} \phi_{\text{Had}}(E)dE$$

Equation 6-1: Calculation of High Energy Hadron Equivalent fluence in FLUKA. The intermediate energy approximation can be derived from factors obtained in measurements characterising SRAM memories [10]

Position 4 (129cm)	Dose [Gy]	1-Mev NEQ cm <sup>-2</sup>	Position 7 (Old, P4 New)	Dose [Gy]	1-Mev NEQ cm <sup>-2</sup>
POT	Error %	Error %		Error %	Error %
Date	Data/FLUKA	Data/FLUKA	POT, Date	Data/FLUKA	Data/FLUKA
7.585e+15	1.73E-14	2.26E-04			
24.11.14	3.9%	1.9%			
27.11.14					
5.618e+15	1.75E-14	1.50E-04			
28.11.14	3.6%	4.9%			
30.11.14					
4.668e+15	1.64E-14	1.98E-04	4.668e+15	1.22E-14	1.45E-04
01.12.14	3.4%	5.9%	01.12.14	2.7%	1.5%
04.12.14			04.12.14		
2.313E+15	1.56E-14	1.68E-04	2.313E+15	1.11E-14	1.07E-04
05.12.14	2.9%	2.9%	05.12.14	3.5%	3.2%
07.12.14			07.12.14		
4.633E+15	1.69E-14	1.23E-04	4.633E+15	1.23E-14	1.12E-04
08.12.14	2.9%	10%	08.12.14	3.1%	4.9%
11.12.14			11.12.14		

<sup>vi</sup> At the time of writing this is performed solely for the case of Toshiba memories [3]

5.722E+15	1.52E-14	1.34E-04
12.12.14	2.7%	14%
15.12.14		

Table 7: Repeated measurements for positions 4 and 7

Positions 4, 7 (Table 7) 11 and 15 (Table 8) show repeated measurements in time for the same position. These positions had distinct mixed field characteristics which were exploited by users during a number of runs. Measurements were followed solely with deported modules, and only TID and  $\Phi_{eq}$  data is available. With a few exceptions, ionising dose measurements are consistent over time for the RadMON and show an agreement mostly within 20-25% of FLUKA. This information excludes the aforementioned case where the V6 measure 40-50% less than the V5 as it will be shown in section 7 for the 2015 measurements, but for the 2014 measurements, it was argued that this showed a good agreement with FLUKA.

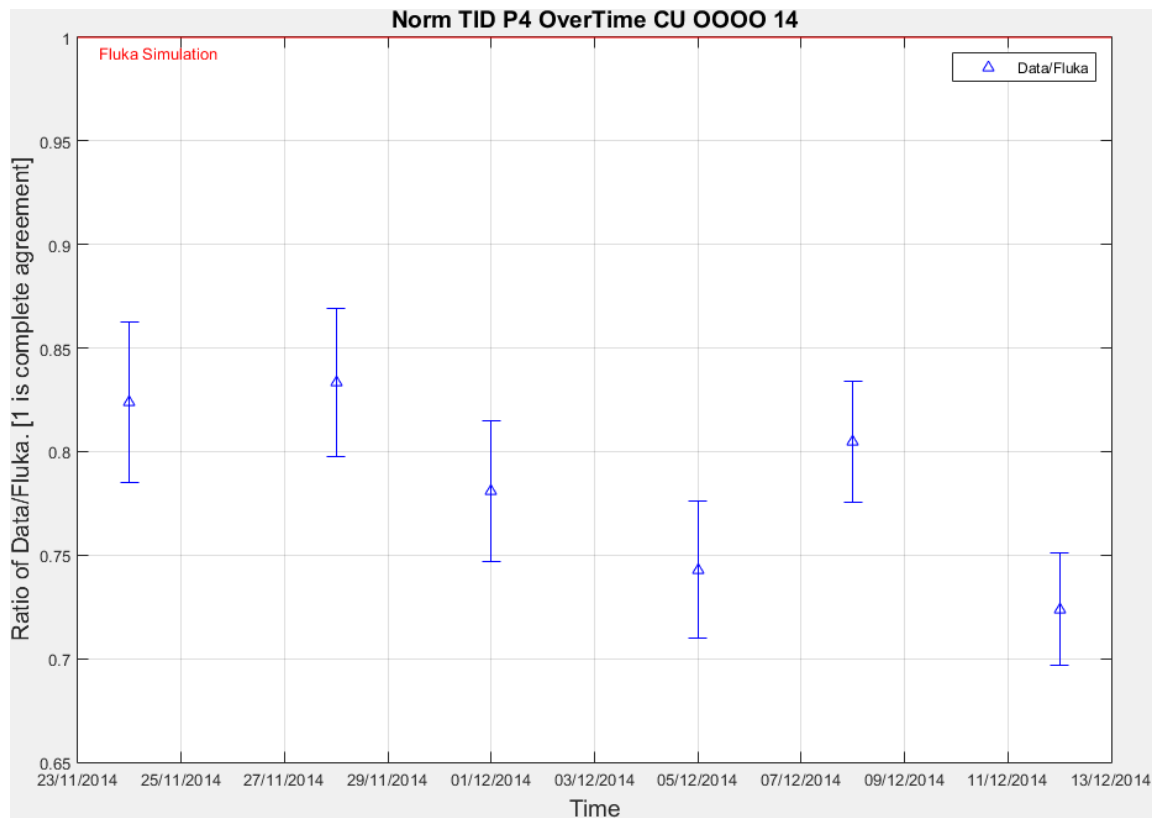


Figure 6-5: Dose measurements on position 4 over the course of 20 days



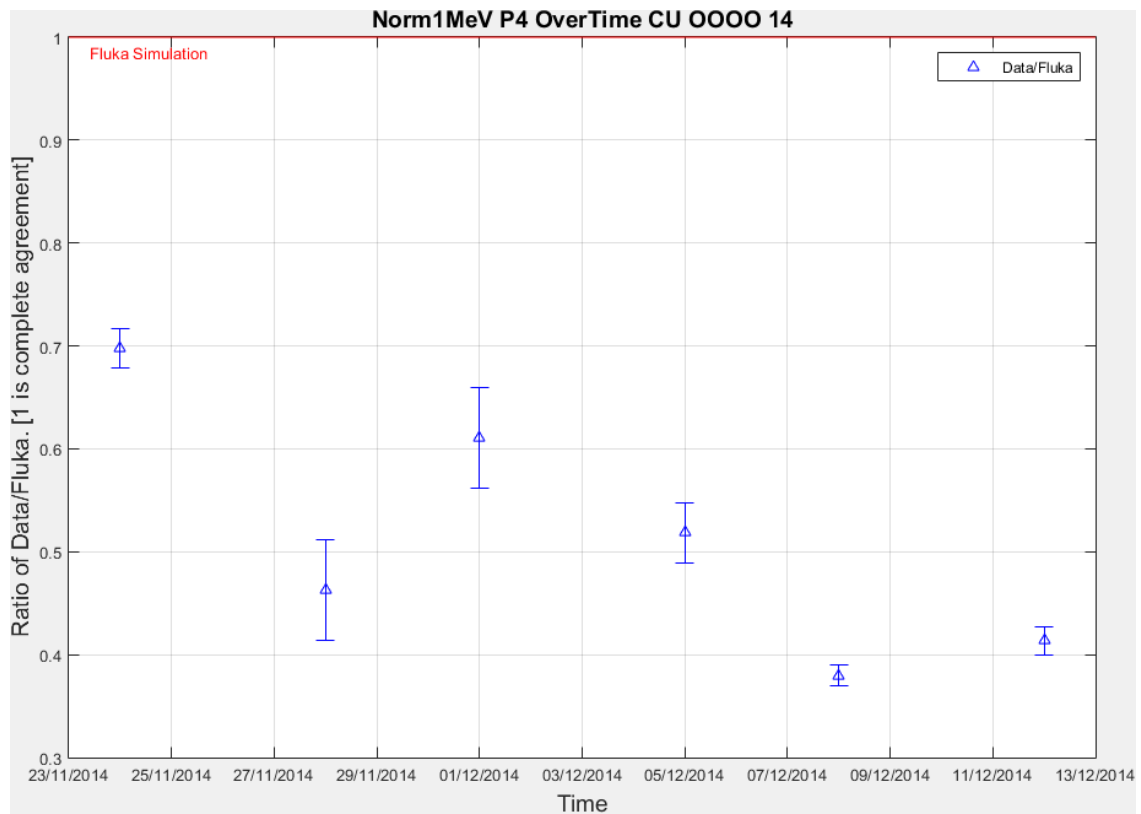


Figure 6-6:  $\Phi_{eq}$  measurements on position 4 over the course of 20 days

Position 11	Dose [Gy]	1-Mev NEQ cm <sup>-2</sup>	Position 15	Dose [Gy]	1-Mev NEQ cm <sup>-2</sup>
Date	Error %	Error %	Date	Error %	Error %
POT	Data/FLUKA	Data/FLUKA	POT	Data/FLUKA	Data/FLUKA
DM2 121 cm			DM4 84 cm		
			7.585e+15	2.88E-14	1.90E-04
			24.11.14	4%	13%
			27.11.14		
			5.618+15	2.78E-14	1.36E-04
			28.11.14	3.2%	13.3%
			30.11.14		
4.668e+15	1.23E-14	8.77E-05	4.668e+15	2.88E-14	1.06E-04
01.12.14	1.9%	4%	01.12.14	2.9%	3.5%
04.12.14			04.12.14		
2.313E+15	1.04E-14	7.04E-05	2.313E+15	2.65E-14	1.36E-04
05.12.14	2.5%	1.5%	05.12.14	2.2%	1%
07.12.14			07.12.14		



4.633E+15	1.45E-14	8.49E-05	4.633E+15	2.68E-14	1.11E-04
08.12.14	2.2%	2.8%	08.12.14	2.1%	4%
11.12.14			11.12.14		
5.722E+15	2.79E-14	1.06E-04	5.722E+15	3.32E-14	1.26E-04
12.12.14	2.1%	9.8%	12.12.14	2%	6.1%
15.12.14			15.12.14		

Table 8: Repeated measurements for positions 11 and 15

Measurements for positions 11 and 15 were performed at 121cm and 84 cm from the floor respectively. The appropriate FLUKA calibration factors were calculated for these heights and compared to measurement. Positions 4 and 15 were during the same period of time, offering insight for a longitudinal position to the beam line, which provides softer spectra (position 4) and a position lateral to the beam line providing harder spectra (position 15). It is seen that similar Data/FLUKA ratios near 70-80% are visible for the TID.

The overall strongest conclusion for the Cu\_OOOO configuration that can be reached is that on average, measured values are consistently lower than simulation on all three radiation field measurement types. Final conclusion on 2014 commissioning lead to an agreement in TID of 20% with FLUKA, to which an inter-RadMON variability of 10% could be appended. This left out further progress into HEH and  $\Phi_{eq}$  benchmarking, which would resume again in 2015. Further information on these differences with simulation and SEC calibration considerations is on chapter **Error! Reference source not found..**

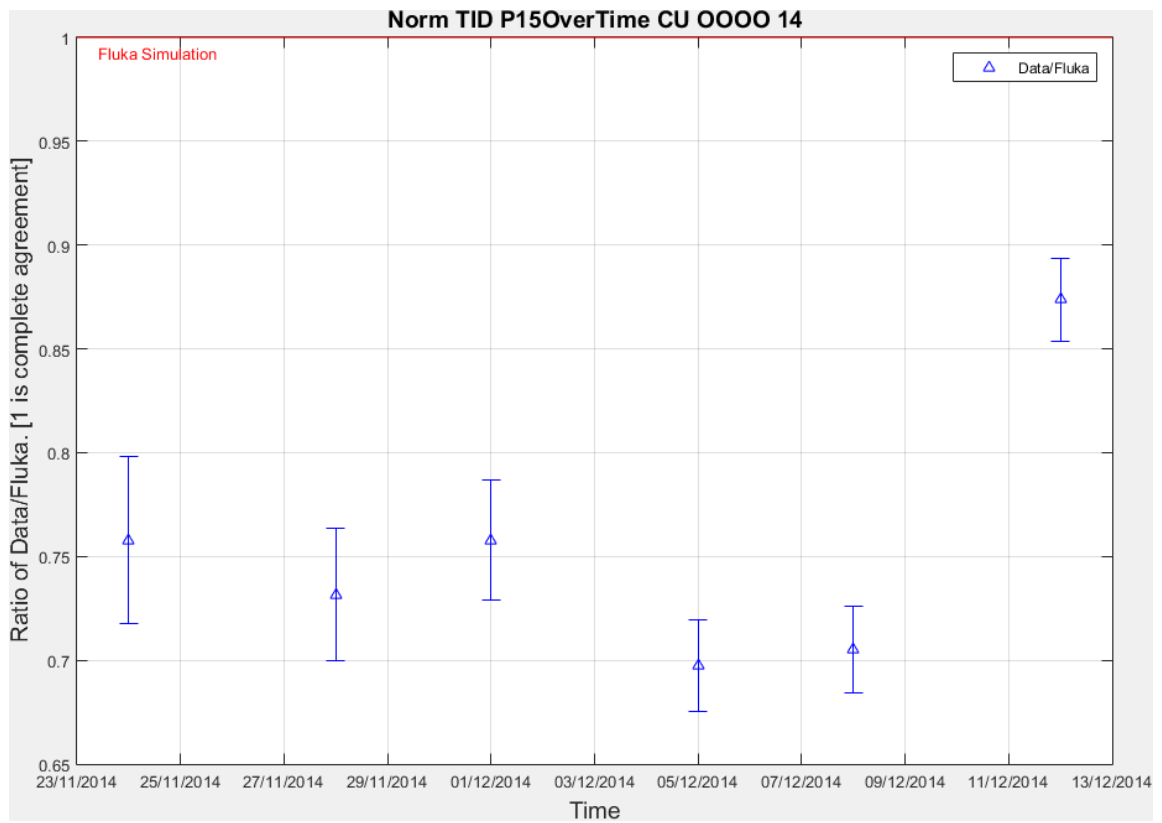


Figure 6-7: Dose measurements on position 15 over the course of 20 days

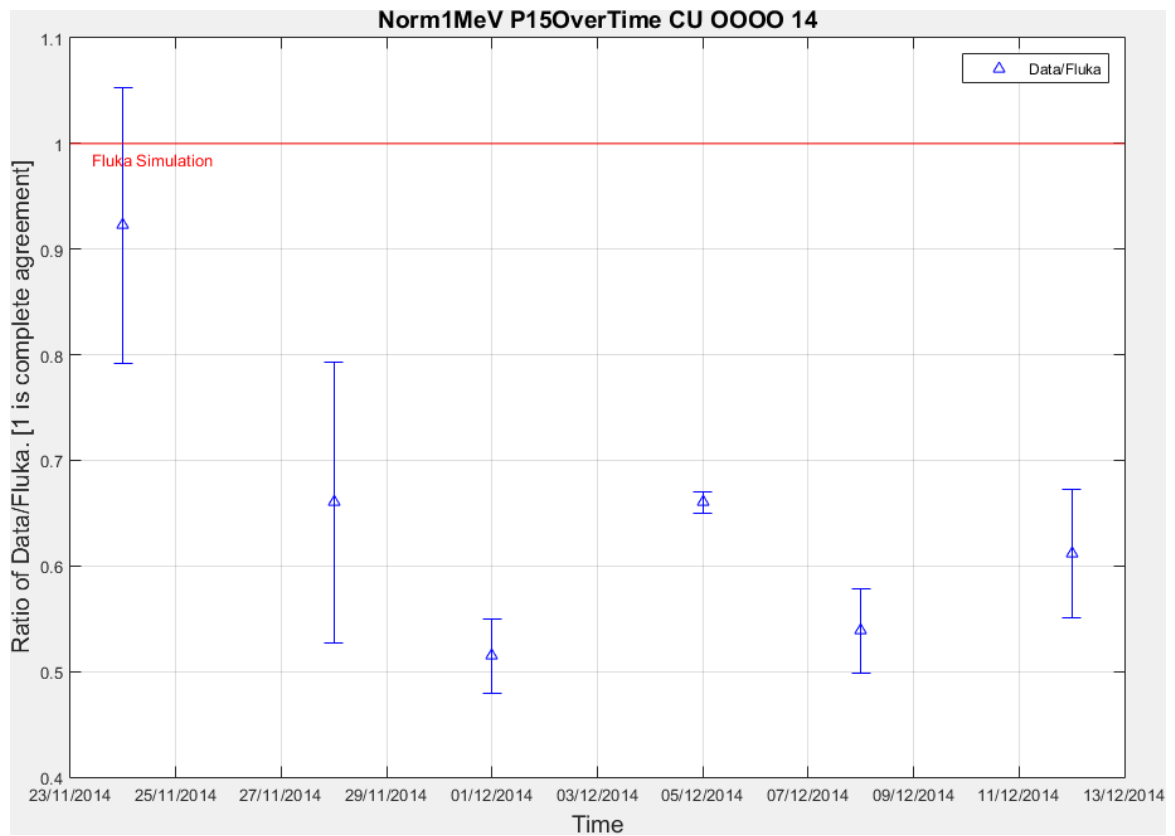


Figure 6-8:  $\Phi_{eq}$  measurements on position 15 over the course of 20 days

## 6.2 Aluminium Holes – AIH OOOO

Position	Dose [Gy]	HEHeq cm <sup>-2</sup>	THeq cm <sup>-2</sup>	1-Mev NEQ cm <sup>-2</sup>	R Factor
	Error %	Error %	Error %	Error %	
	Data/FLUKA	Data/FLUKA	Data/FLUKA	Data/FLUKA	
<b>1</b>	2.28E-15	7.14E-06	3.30E-06	3.22E-05	0.49
<b>MB3+MB6</b>	4%	12.6%		5.7%	
	0.82	1.22		0.45	
<b>3</b>	2.36E-15	4.78E-06	3.27E-06	No measurement made	0.67
<b>400nm</b>	10%	12.7%			
<b>MB2+MB5</b>	0.61	0.61			
<b>3</b>	2.51E-15			1.46E-05	
<b>Height of 10 cm from the floor</b>	10.9%			23%	
	NA			NA	
<b>11</b>	4.58E-15			2.81E-05	
	4.8%			21%	
	0.63			0.74	
<b>14</b>	7.05E-15			2.62E-05	
	6.6%			22.6%	
	0.41			0.49	
<b>15</b>	8.14E-15			3.21E-05	
<b>Height of 10 cm from the floor</b>	8.9%			3.1%	

Table 9: Data set for AIH\_OOOO measurements with independent RadMON R factor

One example of how the R factor measurement was carried out can be seen in figure 6-9 where two motherboards with memories biased at 3V and 5V are placed in position 3 to make a measurement. It is recommended to perform repeated measurements in this configuration again. This same approach was taken in 2015 measurements when investigating R factor measurements between V5 and V6.

There is a small positioning error as the memories are not strictly together due to the metal casings, however it is argued that this error is rather small due to predictions from simulation [1] showing that this is an acceptable admission due to in most positions the field only varying in 10% per meter. Measurements at different heights in the same position also showed that this difference was not larger than 15%.



Figure 6-9: AIH\_OOOO R factor measurement on P3

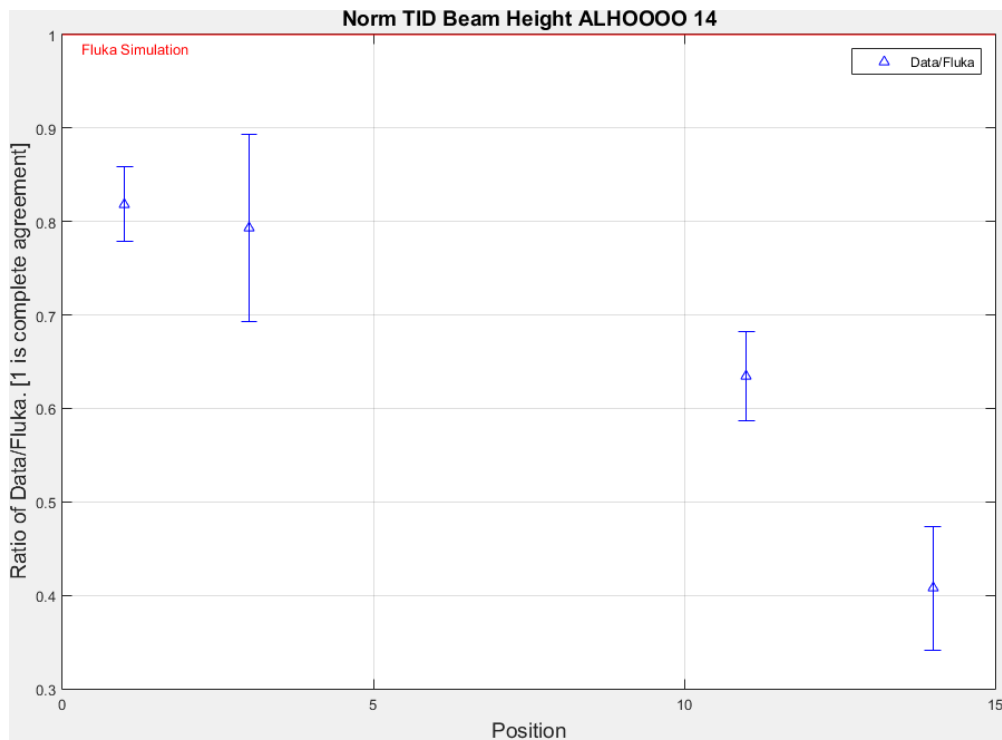


Figure 6-10: Agreement between TID measurement and simulation for AIH\_OOOO

As shown by the figure above with single measurements, further investigation should be done on the harder spectra of the AIH\_OOOO configuration.

### Copper full shielding - CIIC

A short run on this configuration was performed on 19<sup>th</sup> of November where only three deported modules were present. Only three deported modules were used in this run. It is presented here for completeness.

Position	Dose [Gy]	1-Mev NEQ cm <sup>-2</sup>
Done 18.11.14	Error %	Error %
	Data/FLUKA	Data/FLUKA
3 beam height	4.15E-16	$\Delta V_{th}$ is 0
	1.3%	No $\Phi_{eq}$ measured
	FLUKA not available	
3 floor	3.51E-16	1.28E-05
	14.6%	40%
	FLUKA not available	FLUKA not available
15 floor	3.93E-15	4.26E-05
	13.9%	7%
	FLUKA not available	FLUKA not available

Table 10: Small CU\_CIIC run with measurements

### 6.3 Measurements on the MONTRAC during 2014 Commissioning Period

Day of test <sup>vii</sup>	RadMON <sup>viii</sup>	Beam Type
31 October	DM6+DM2	Intensity scan of beam
3 November	DM6+DM2	Direct beam with no target
17 Nov	ESA SEU monitor+MB1+DM5	Blown up beam
18 Nov	DM6	Blown up beam
1 Dec	DM1	Beam impinging on copper target
5 Dec	DM1	Beam impinging on copper target
8 Dec	DM1	Beam impinging on copper target
12 Dec	DM1 15 short circuit RadFET board	Beam impinging on copper target

Table 11: Montrac measurements during the 2014 commissioning period

There were extensive measurements on the Montrac for direct beam, expanded beam FWHM and beam after impinging on copper target.

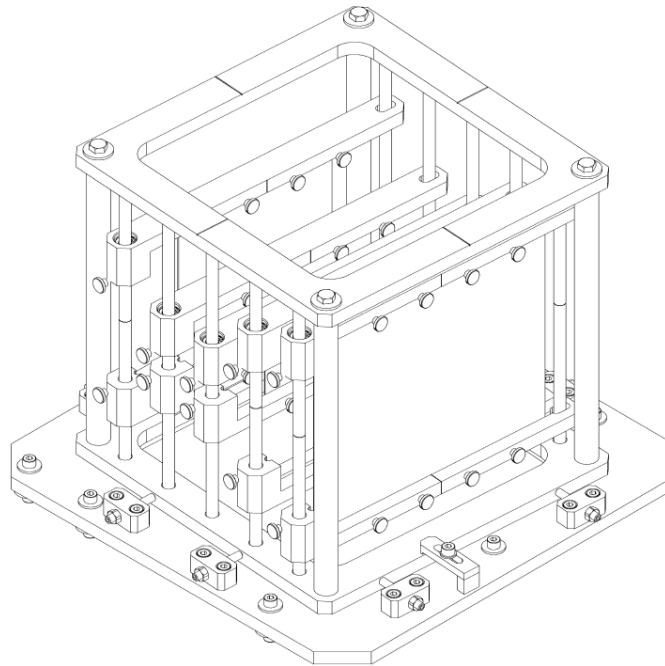


Figure 6-11 Technical drawing of the Montrac. It allows the placement of 5 electronic boards in parallel. It is angled to the left due to the path of the beam (see Figure 5-1)

The first setup involved testing two deported modules, (DM6 placed on the BTV and DM2 placed on the Montrac) to investigate the difference between the response of the 100nm and 400nm

<sup>vii</sup> Precise timings detailed in tables 12-17

<sup>viii</sup> Detailed position information on tables 12-17

radfets in a pulsed beam. No conclusions of this study have been made due to the high gradient of the beam dose rate when no target is used.

Montrac scan testing during 2014 ( 31 october)						
Run	Split Start	Split End	Intensity per spill	POT	RadFET of DM6 Centred on Beam	RadFET of DM2 Centred on Beam <sup>ix</sup>
1	14:09	15:00	1E11	3.78E12	400nm	100nm
2	15:01	15:25	5E10	5.30E11	400nm	100nm
3	15:26	16:00	3E10	5.80E11	400nm	100nm
4	16:10	16:31	5E09	1.00E11	400nm	100nm
5	19:06	22:19	1E11	1.75E13	100nm	100nm

Table 12: Setup of the scan testing on the Montrac for 31<sup>st</sup> of October

Montrac scan testing during 2014 ( 31 October)			
Deported module	Run (see table above)	Dose [Gy]	1-Mev NEQ cm <sup>-2</sup>
DM2 100 nm Montrac	1	1.10E-10	7.75E-02
	2	1.13E-10	6.88E-02
	3	1.15E-10	6.75E-02
	4	1.15E-10	6.55E-02
	5	6.78E-11	6.57E-02
DM6	1 (400nm)	6.69E-11	8.42E-02
BTV	2 (400nm)	6.36E-11	8.15E-02
(Before Target Table)	3 (400nm)	6.69E-11	8.55E-02
	4 (400nm)	6.97E-11	8.84E-02
	5 (100nm)	9.06E-11	8.50E-02

Table 13: Intensity scan results for deported modules on the 31 October run

The two tables above detail the intensity scan test where it was attempted to perform irradiation down to 5E9 protons per spill from the PS. In run 5, the deported module in front was moved to so that the beam would be centred on the 100nm thick oxide RadFET on DM6. The responses are different in the last run for both deported modules and the 100nm RadFET on the Montrac measures more than the 400nm upstream. This observed difference is due to the large gradient at this position [3] A small variation in the positioning can induce a large variation on the TID measurement. As one deported module was located on the BTV screen and another in the Montrac location, it is likely that there is a small error on the centering of both RadFETs. On the other hand, the  $\Phi_{eq}$

<sup>ix</sup> Deported module 2 only had one 100nm RadFET

is comparable for both, also seen in table 13. A reversal is seen on run 5 when the DM on the BTV<sup>x</sup> is positioned to focus on the 100nm, where it measures more with a smaller difference of only 25%. As there are three PIN diodes in a horizontal row on each RadMON, a small variation in the DM positioning will not induce such a difference for the 1-MeV neutron equivalent fluence as for the TID measurement.

#### Montrac testing during 2014

Date in	Config	RadMON system	Dose [Gy/POT]	1-Mev NEQ cm <sup>-2</sup>
Date out	Centred on		Error %	Error %
POT	Rfet=R PIN=P		Data/FLUKA	Data/FLUKA
3.11.2014 21:18	No-target Beam	DM2	1.29E-10	5.12E-02
3.11.2014 23:01	R100nm	Downstream	3.7%	7.5%
1.56E+13	Intensity/spill: 1E11	on Montrac		
3.11.2014 21:18	No-target Beam	DM6	2.09E-10	4.93E-02
3.11.2014 21:27	R100nm	10 minutes	3.2%	9.6%
1.56E+13	Intensity/spill: 1E11	Upstream on BTV		

Table 14: Direct beam with no target measurements

Date in	Config	RadMON system	Dose [Gy/POT]	SEU's
Date out	Centred on		Error %	HEH
POT	Rfet=R PIN=P		Data/FLUKA	
17.11.2014 11:56	Blown up Beam	MB1	3.40E-12	18'038 SEU counts <sup>xi</sup>
17.11.2014 12:01	Center of Memories	17 spills	11.6%	Norm HEH fluence:
6.31E+12	400nm RadFET			1.04E-03 cm <sup>-2</sup>
Date in	Config	RadMON system	Dose [Gy/POT]	1-Mev NEQ cm <sup>-2</sup>
Date out	Centred on		Error %	Error %
POT	Rfet=R PIN=P		Data/FLUKA	Data/FLUKA
17.11.2014 11:56	Blown up Beam	DM5	3.26E-12	1.11E-02
17.11.2014 12:01	Between center of radfets	17 spills	10%	20%
6.31E+12		In front of MB1		

Table 15: Blown up beam configuration measurements

<sup>x</sup> Beam TV (ref)

<sup>xi</sup> HEH measurement included only for this specific run with Motherboard testing



Date in Date out POT	Config Centred on Rfet=R PIN=P	RadMON system	Intensity	Dose [Gy/POT]
18.11.2014 13:42	Blown up Beam	DM6	5.00E+11	3.23E-12
18.11.2014 14:38	100nm RadFET		3.50E+11	2.92E-12
4.57E+13	Intensity scan		2.00E+11	2.89E-12
			5.00E+11	2.87E-12

Table 16: Blown up beam configuration with intensity scan

Date in Date out POT	Config Centred on Rfet=R PIN=P	RadMON system	Dose [Gy/POT] Error % Data/FLUKA	1-Mev NEQ cm <sup>-2</sup> Error % Data/FLUKA
01.12.2014 13:35	Copper target	DM1	2.73E-13	7.47E-04
04.12.2014 14:38 4.68E+15	Between center of radfets	100nm	2.4%	2.9%
05.12.2014 13:42	Copper target	DM1	1.64E-13	1.32E-13
07.12.2014 14:38 2.32E+15	Between center of radfets	100nm x2	4.7%	5.7%
08.12.2014 13:42	Copper target	DM1	1.72E-13	1.32E-13
11.12.2014 14:38 4.63E+15	PIN diode	100nm x2	2%	2.7%
12.12.2014 13:42	Copper target	100nm x2 (swapped)	2.51E-13	2.27E-13
15.12.2014 14:38 5.72E+31	Single PIN diode		1.7%	1.6%

Table 17: Montrac measurements using deported modules during 2014 commissioning

### 6.3.1 Short circuited Radfet card

RadFET's can be short circuited and deployed independently from a RadMON. This allows for point measurements without the need of installing a RadMON. Its therefore very simple to install such RadFETs, however the drawback is that this is a single point measurement, i.e the TID is only measured at the end of the irradiation and measurement is recorded on-line during the run. The RadFETs are therefore read after the run by a surrogate RadMON system. An example of a RadFET grid that has been placed at the Montrac test location to evaluate the dose profile at this location is shown below. Please refer to Figure 7-11 on the left for a photograph of this grid.

Montrac RadFET board on Run Cu OOOO on 12.12.14				Distance from center (mm) <sup>xii</sup>
Start:	1.51E-13	1.55E-13	1.13E-13	20mm
	0.74	0.76	0.56	
12.12.14	1.84E-13	1.85E-13	1.31E-13	10mm
	0.91	0.91	0.65	
15:36:00	1.99E-13	2.03E-13	1.41E-13	0
	0.98	1.00	0.69	
End:	1.95E-13	1.98E-13	1.36E-13	10mm
	0.96	0.98	0.67	
POT:	1.71E-13	1.72E-13	1.25E-13	20mm
	5.72E+31	0.84	0.85	
Distance from center (mm)	18 mm	0	18 mm	

Table 18: Normalised dose factors for short circuit RadFET grid. The grid was installed at the Montrac test location to evaluate the beam profile at this location using the copper target

Firstly, Table 18 portrays a geometrical result which was confirmed in further measurements where the beam intensity is distributed in favour of the left side when looking downstream. In this single measurement, the center-right radfet accrued 30% less than the one in the center and center-left. A similar ratio is seen at the edges. Their ratio with the radfet in the center is shown below the normalised dose (center is normalised to unity). Despite in most cases the beam profile appearing mostly uniform on the MWPC, it seems the energy is not distributed evenly. These types of tables were coloured linearly using Excel's conditional formatting tool.

<sup>xii</sup> Measured from the center of the central RadFET to the center of the RadFET in question

## 6.4 2014 Commissioning period overview

The CHARM start-up in October 2014 until December 2014 was successful. Learning how run the facility effectively, working with IRRAD and the PS and co-ordinating data measurement were important points in 2014 from which the CHARM team learned a lot and carried on onto 2015. All CHARM systems had to be debugged at one point and this also took time to master.

The 2014 commissioning period was transitioned into user testing runs where the highest flux rates were on demand, thus leading to an asymmetrical data set towards Cu\_OOOO. This provided good insight for experiment planning on this configuration, to the benefit of the users, at the cost of data for the other testing configurations.

In these circumstances, the RadMON motherboards were seldom used, this still possible by the lower PS beam intensity at 1E11 during the 12.11.2014 test. The asymmetry in the data set was enhanced by the large progress of short circuited radfet measurement<sup>xiii</sup>, where extensive analysis was made in the center of the beam and in parallel by I. Toccafondo (ref) around the vicinity optical fibers for dosimetry.

### 2014 Result summary tables (averages)

Official 2014 Positions	TID Error Data/FLUKA	HEHeq Error Data/FLUKA	Theq Error Data/FLUKA	1-Mev NEQ Error Data/FLUKA	R factor Error Data/FLUKA
1 D/F	2.28E-15 4% 0.92	7.14E-06 12.6% 1.22	3.30E-06	3.22E-05 5.7% 0.45	0.49
3 D/F	2.36E-15 10% 0.61 (400nm)	4.78E-06 12.7% 0.61	3.27E-06	Measurement not performed	0.68
11 D/F	4.58E-15 4.8% 0.63			2.81E-05 21% 0.74	
14 OLD D/F	1.47E-14  0.85			2.62E-05  0.49	

Table 19 Summary of 2014 AIH OOOO results

<sup>xiii</sup> A record of these measurements can be found on (Philippe files)

Official 2014 Positions	TID Error Data/FLUKA	1-Mev NEQ Error Data/FLUKA
3 beam D/F	4.15E-16 1.3%	No change
3 OLD floor D/F	3.51E-16 14.6%	1.28E-05 40%
15 floor D/F	3.93E-15 13.9%	4.26E-05 7%

Table 20 Short CU CIIC run

	TID	Sample $\sigma$ error	1-Mev NEQ	Sample $\sigma$ error
No target beam D/F	1.19E-10	35%	6.63E-02	18%
BuB D/F	3.10E-12	7%	1.11E-02	Single result
Copper target interaction D/F	1.80E-13	27%	5.48E-04	34%

Table 21: Montrac averages normalised by POT. FLUKA data available soon.

Standard deviation shows most consistent measurements for the blown up beam. This could be in part due to the ease of aligning a dosimeter to the center of the Montrac test box.



Official 2014 Positions	TID Data/Fluka	Sample error for repeated samples	$\sigma$ for HEHeq	1-Mev NEQ	Sample error for repeated samples
1 (1 new) Single	7.92E-15 4.5% 0.65			2.17E-04 12.3% 0.73	
3 old Single	2.64E-14 9.4% 1.45		4.39E-05 12.7% 0.90	3.75E-04 23.4% 1.15	
4 old Repeated	1.65E-14 6% 0.78	6%		1.67E-04 24% 0.51	24%
7 old Repeated	2.66E-14 7% 0.63	48%	5.29E-05 12.7% 0.96	1.36E-04 25% 0.58	25%
11 (8new) Repeated	2.43E-14 8% 0.67	40%	3.83E-05 12.7% 0.80	1.75E-04 44% 0.53	44%
14 Repeated	1.56E-14 3.3% 0.63			8.61E-05 6.3% 1.02	
15 (84cm) Repeated	3.30E-14 9.8% 0.71	9%	6.22E-05 12.7% 0.73	1.86E-04 24% 0.71	24%
16 Single	2.69E-14 4.5% 0.61			1.33E-04 4% 0.60	
19 (13 new) Single	3.73E-14 5.3% 0.97			2.15E-04 7.7% 0.98	

Table 22: Summary of 2014 CU OOOO results

## 7. 2015 RESULTS

The 2015 commissioning period ran from 18 May 2015 till 10 June 2015. The variety and quantity of the data increased across different configurations, partially aided by the ability of the RadMON V6 to measure the R factor with one motherboard unit as explained in section 4.2.4. There was an emphasis in symmetry and cross checking the variability between different RadMON systems for measurements in the same positions.

In the following chapter, results are presented by facility configuration. Attention is drawn to the fact that the position scored in FLUKA were changed from 2014 to 2015, as seen in figure **Error! Reference source not found..** For every measurement, an effort was made to position both the motherboard and the deported module of each respective RadMON system together in terms of dose, 100nm RadFET measurements remain the reference as explain in section 4.2.3.

In addition, two V5 motherboards were kept together in order to perform R factor measurements by biasing one set of Toshiba memories at 5V and the other at 3V, see Figure 7-1 Positions 1 and 2 with . Unless otherwise stated all results are from RadMON V6. The prevailing pattern in this commissioning period was the discrepancy between total ionising dose measurements between the V5 and the V6, which is still under review. New data on the SEC calibration factor [2] has led to a new ongoing investigation on how this could the overall data set. For all the results presented in this report, the SEC calibration factor used is of 2.24E7 protons per count.

### 7.1 Impact of Cypress intermediate neutron response on HEHeq simulation

A preliminary study by R.G. Alia showed that the agreement between the Cypress and simulated HEHeq is in fact in much closer agreement if one considers the Cypress response to intermediate neutrons. This pushes the average 60% HEH agreement with FLUKA in full shielding up to 70-80% in most cases. This will be applied in future Cypress measurements, where the full effect on the R factor should also be checked. Thus this is adopted and used in the summary tables below. [10]

Position	Full shielding HEHeq/ HEHeqV6	No shielding HEHeq/ HEHeqV6	Position	Full shielding HEHeq/ HEHeqV6	No shielding HEHeq/ HEHeqV6
1	1.19	1.28	6	1.19	1.14
2	1.18	1.27	7	1.19	1.12
3	1.15	1.18	8	1.18	1.11
4	1.16	1.15	9	1.18	1.11
5	1.18	1.15	10	1.16	1.09

Table 23: Increment factors on simulated HEHeq values from Toshiba to Cypress SRAM

## 7.2 Aluminium no shielding – Al\_OOOO

Run time: 18/05/2015 20:00:00 to 20/05/2015 05:59:20 POT: 2.085E15

Position	Dose [Gy]	HEHeq <sup>xiv</sup> cm <sup>-2</sup>	THeq cm <sup>-2</sup>	1-Mev NEQ cm <sup>-2</sup>	R Factor
<b>1</b>	<b>Error %</b>	<b>Error %</b>	<b>Error %</b>	<b>Error %</b>	
	<b>Data/FLUKA</b>	<b>Data/FLUKA</b>		<b>Data/FLUKA</b>	
<b>V6 (DM7+MB7)</b>	2.42E-15	8.95E-06	8.98E-06	5.42E-05	1.01
	11.9%	10.6%		45%	
	0.58	0.90		0.98	
<b>V5 (MB5+MB3)</b>	3.30E-15 <sup>xv</sup>	9.27E-06	4.65E-06	Not measured	0.52
	10%	10.6%			
	0.79	0.93			

Table 24: Measurements on Position 1 with V5 and V6

The high error on the 1-MeV NEQ measurement is due to the lower fluences in this facility configuration. The 1-MeV neutron equivalent fluence measured in position 1 by RadMON V6#7 is 1.19E11 whilst in order to obtain an error of 10% the PIN diodes must be irradiated up to 1.62E12 1-MeV neutron equivalent particles per cm<sup>2</sup>. During 2014 the aluminium target was moved out of the target for a maintenance operation. Thus the priority for the Al\_OOOO measurement was to obtain initial TID and Risk factor data.

There is a factor of 2 between  $\Phi_{eq}$  measurements of the RadMON V6 and V5, whilst the HEH measurements are very similar. This recurring effect is being investigated. tables

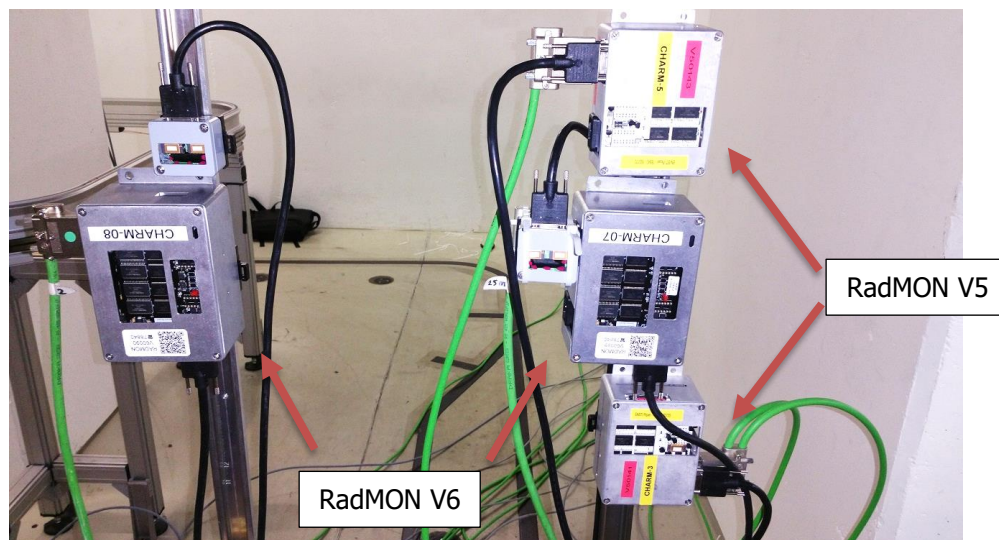


Figure 7-1 Positions 1 and 2 with V6#7 motherboard at beam height and motherboards V5#3 and V5#5 above and below. DMV6#7 is at the side of MBV6#7.

<sup>xiv</sup> HEHeq for simulations considering intermediate neutron energy for the RadMON V6. See table 36.

<sup>xv</sup> Only 400nm RadFET measurement available from Motherboard V5#3

	Dose [Gy]	HEHeq cm <sup>-2</sup>	THeq cm <sup>-2</sup>	1-Mev NEQ cm <sup>-2</sup>	R Factor
	Error %	Error %	Error %	Error %	
	Data/FLUKA	Data/FLUKA	Data/FLUKA	Data/FLUKA	
<b>Position</b>	2.82E-15	8.30E-06	1.18E-05	6.20E-05	1.38
<b>2</b>	16.5%	10.6%	8.7%	46%	
<b>V6 (DM8+MB8)</b>	0.60	0.78		1.08	
<b>Position</b>	6.02E-15	1.55E-05	1.30E-05	5.45E-05	0.83
<b>3</b>	6.3%	10.6%	8.7%	45%	
<b>V6 (DM3+MB3)</b>	0.61	0.85		0.78	
<b>Position</b>	5.03E-15	1.55E-05	1.15E-05	5.54E-05	0.74
<b>5</b>	18%	10.6%	8.7%	45%	
<b>V6 (DM4+MB4)</b>	0.47	0.86		0.85	
<b>Position</b>	7.32E-15	1.79E-05	1.17E-05	6.24E-05	0.64
<b>7</b>	7%	10.6%	8.7%	43%	
<b>V6 (DM5+MB5)</b>	0.60	0.87		0.96	

Table 25: Normalised data for positions 2-7 for the AI\_OOOO configuration

Position	Dose [Gy]	HEHeq cm <sup>-2</sup>	THeq cm <sup>-2</sup>	1-Mev NEQ cm <sup>-2</sup>	R Factor
9	Error %	Error %	Error %	Error %	
	Data/FLUKA	Data/FLUKA		Data/FLUKA	
<b>V6 (DM6+MB6)</b>	7.80E-15	1.63E-05	1.34E-05	6.73E-05	0.69
	17%	10.6%	8.7%	42%	
	0.60	0.92		1.08	
<b>V5 DM3<sup>xvi</sup></b>	1.04E-14	Not measured	Not measured	1.06E-04	Not measured
	9%			1.71	
	0.81				

Table 26: Results for AI\_OOOO on position 9 using both V5 and V6

The first sign that the TID measurements on the V5 and the V6 were quite different can be seen on Table 26. Whereas on average V6 TID measurements scored consistently at 50-60% of simulation, the V5, like in 2014, stands closer to the simulation (Table 24, Table 26). Figure 7-2 1 MB V6 with DM6 plus displays a pattern often seen in TID and HEH measurements where in the first positions the measurement is above simulated

<sup>xvi</sup> Unfortunately due to a technical error there is no data available for deposited module #5 V5 in this run



values which can be attributed in part to the lower statistical uncertainty in the simulation due to the lower radiation flux in the area.

Figure 7-4 and Figure 7-5 show close agreement with simulation at consistent ratios for different positions. Ans The R factor varies little for each position, and the difference between position 1 and 2 warrant repeat measurements.

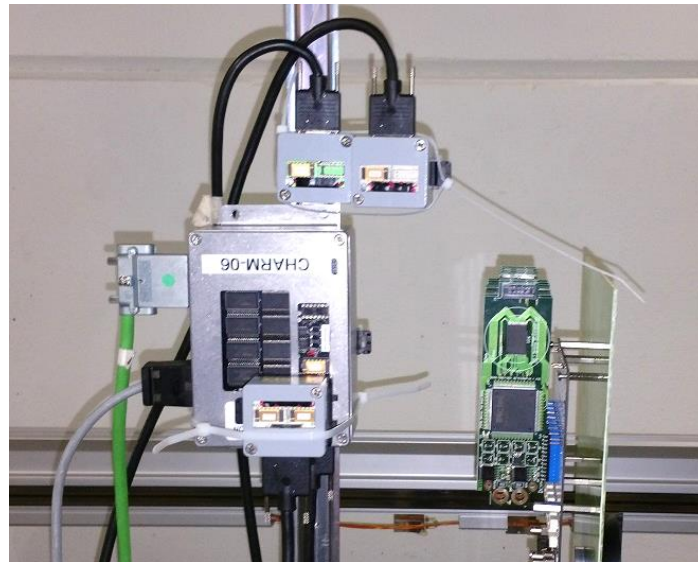


Figure 7-2 1 MB V6 with DM6 plus V5DM#3 and V5DM#5 above

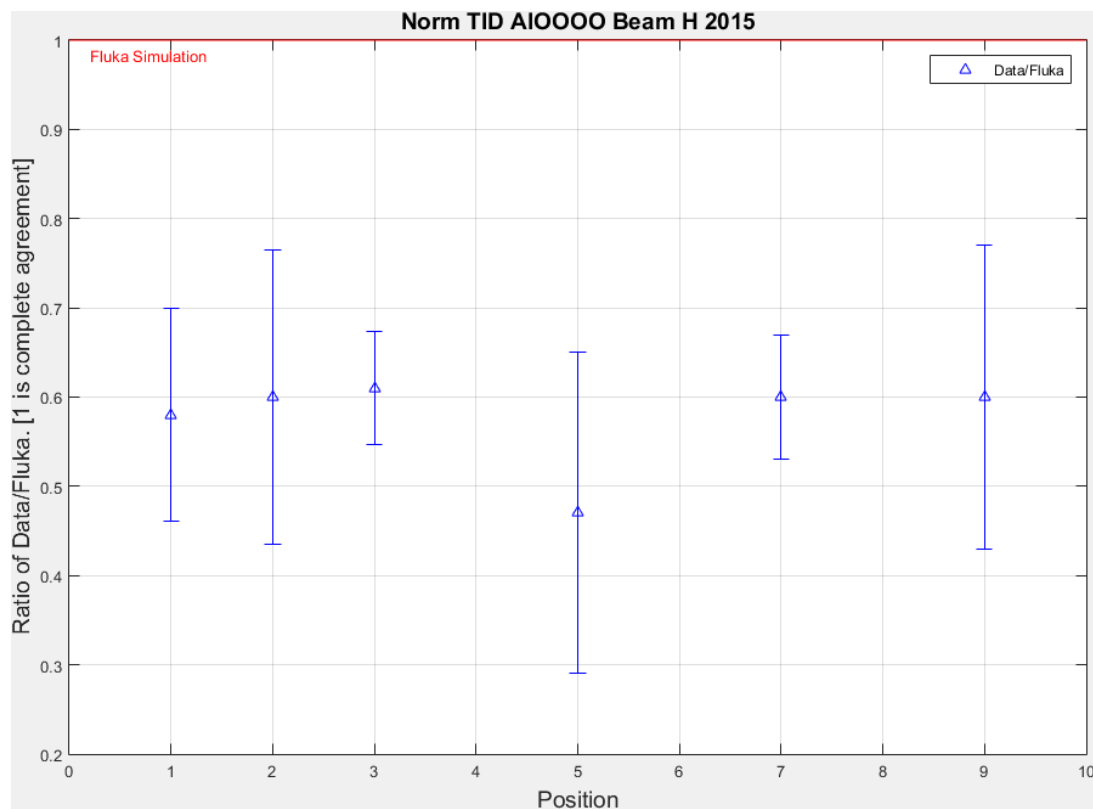


Figure 7-3: Agreement between V6 data and simulation on TID for AI\_0000

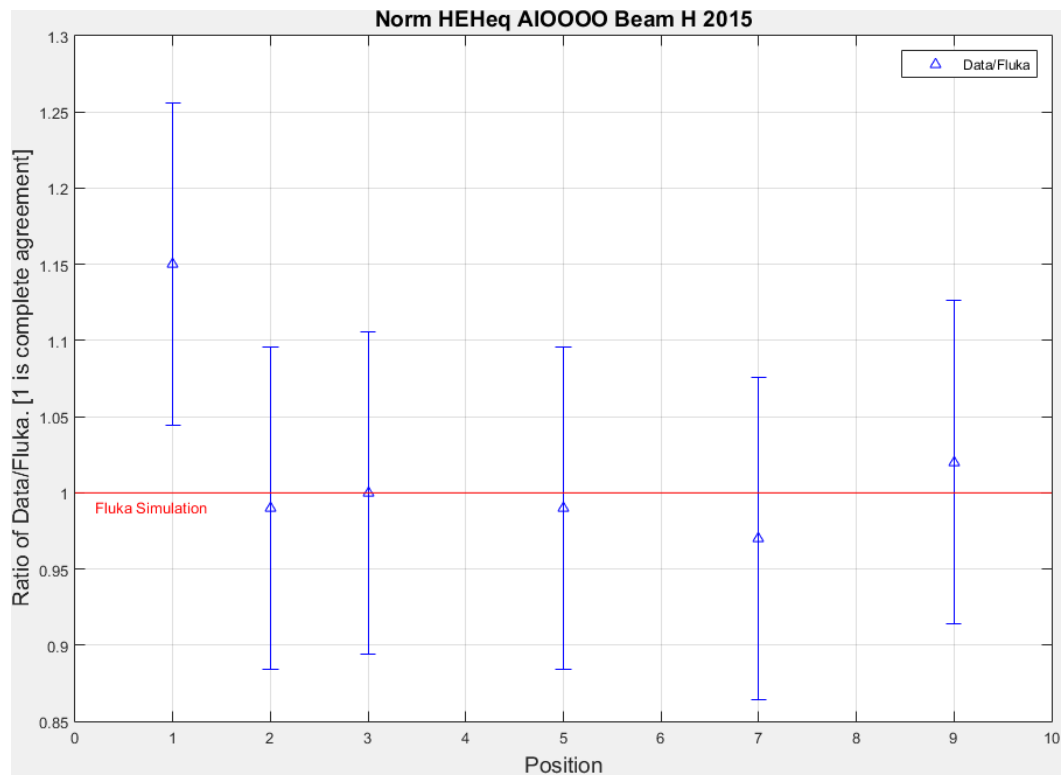


Figure 7-4: Agreement between V6 data and simulation on HEHeq for AI\_O000 using new factors as described in section 7.1

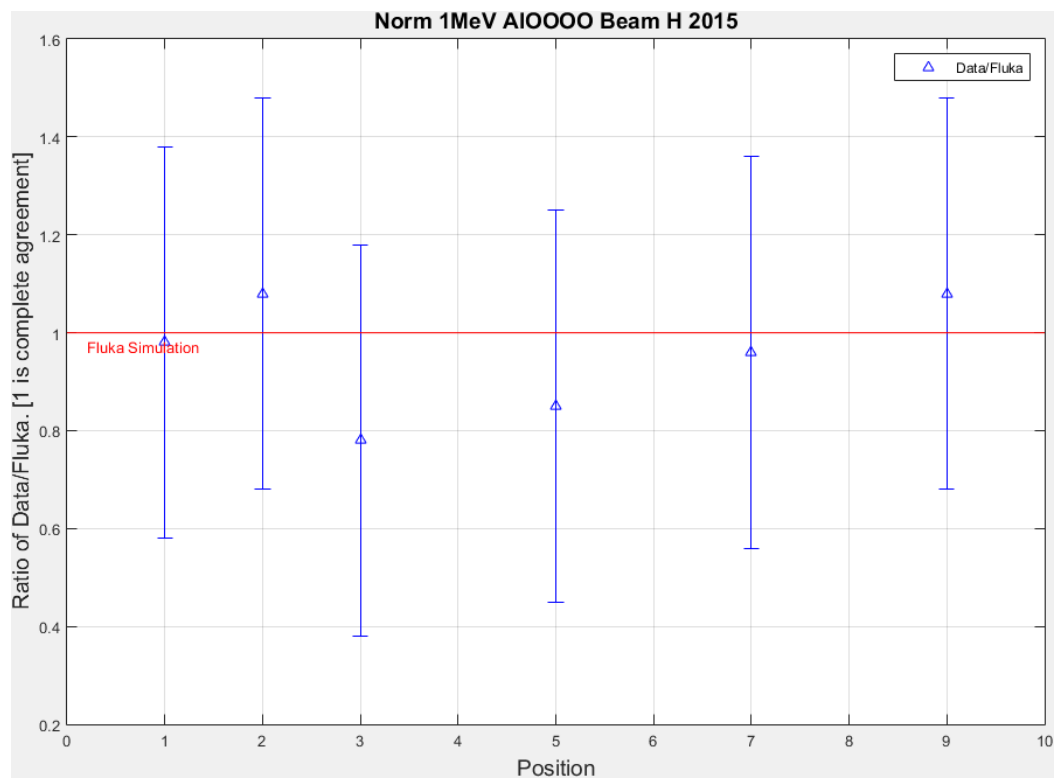


Figure 7-5: Agreement between 1-MeV neutron equivalent fluence measurements and simulation on  $\Phi_{eq}$  for AI\_O000

### 7.3 Copper full shielding – Cu\_CIIC

Run time: 22/05/2015 11:04:00 to 25/05/2015 20:27:40 – POT: 5.548E15

Position	Dose [Gy]	HEHeq cm <sup>-2</sup>	THEq cm <sup>-2</sup>	1-Mev NEQ cm <sup>-2</sup>	R Factor
<b>1</b>	Error %	Error %		Error %	
	Data/FLUKA	Data/FLUKA		Data/FLUKA	
<b>V6 (DM7+MB7)</b>	4.67E-16	1.34E-06	2.73E-05	1.12E-05	15.29
	12.5%	11.3%		30.3%	
	0.69	0.86		0.56	
<b>V5 (MB5+MB3)</b>	Data not available, gateway network error due to FESA class <sup>xvii</sup> maintenance				

Table 27: Normalised results for P1 on Cu\_CIIC configuration. V5 results not available.

	Dose [Gy]	HEHeq cm <sup>-2</sup>	THEq cm <sup>-2</sup>	1-Mev NEQ cm <sup>-2</sup>	R Factor
	Error %	Error %	Error %	Error %	
	Data/FLUKA	Data/FLUKA		Data/FLUKA	
<b>Position</b>	4.82E-16	1.51E-06	3.03E-05	1.12E-05	18.32
<b>2</b>	11%	10.8%		24.4%	
<b>V6 (DM8+MB8)</b>	0.64	0.74		0.56	
<b>Position</b>	7.60E-16	2.74E-06	2.01E-05	2.32E-05	10.81
<b>3</b>	6.5%	10.7%		24.5%	
<b>V6 (DM3+MB3)</b>	0.58	0.69		0.67	
<b>Position</b>	1.00E-15	2.94E-06	2.79E-05	2.82E-05	9.47
<b>5</b>	6.4%	10.6%		40%	
<b>V6 (DM4+MB4)</b>	0.57	0.72		0.69	
<b>Position</b>	1.18E-15	3.45E-06	2.92E-05	2.82E-05	7.59
<b>7</b>	6.2%	10.6%		40%	
<b>V6 (DM5+MB5)</b>	0.58	0.76		0.69	
<b>Position</b>	1.18E-15	4.36E-06	2.81E-05	4.59E-05	6.98
<b>9</b>	3.5%	10.7%		21.3%	
<b>V6 (DM6+MB6)</b>	0.58	0.85		0.96	

Table 28: Normalised results for positions 2-9

<sup>xvii</sup> Refer to [5] for an explanation of the RadMON logging FESA class

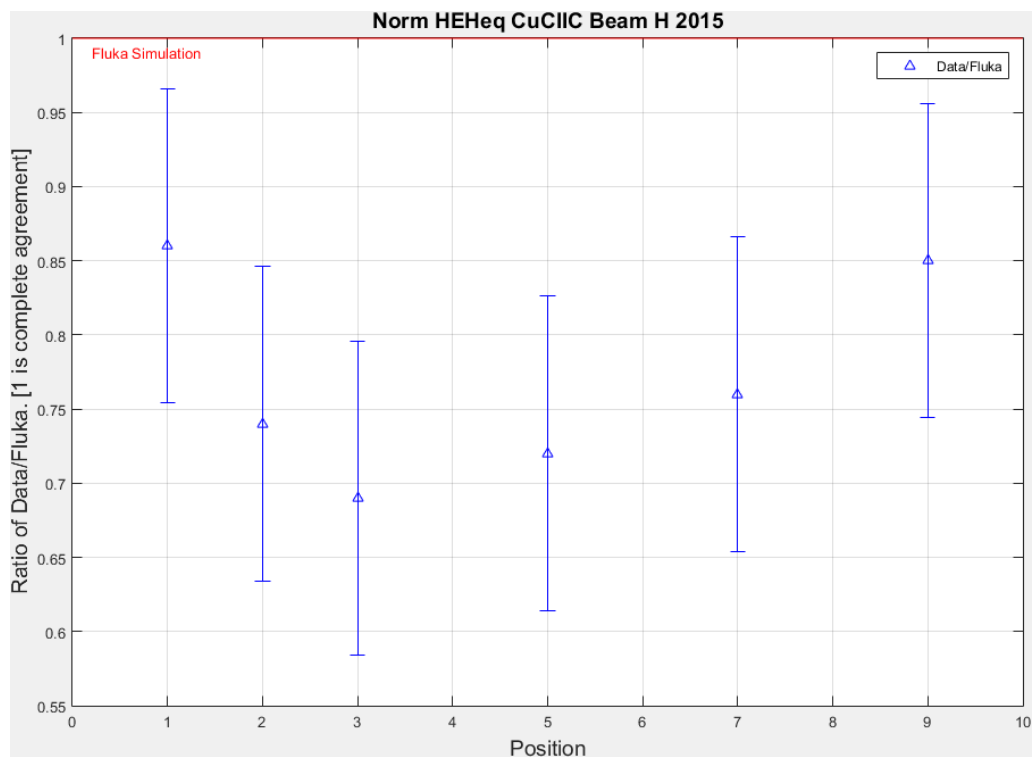
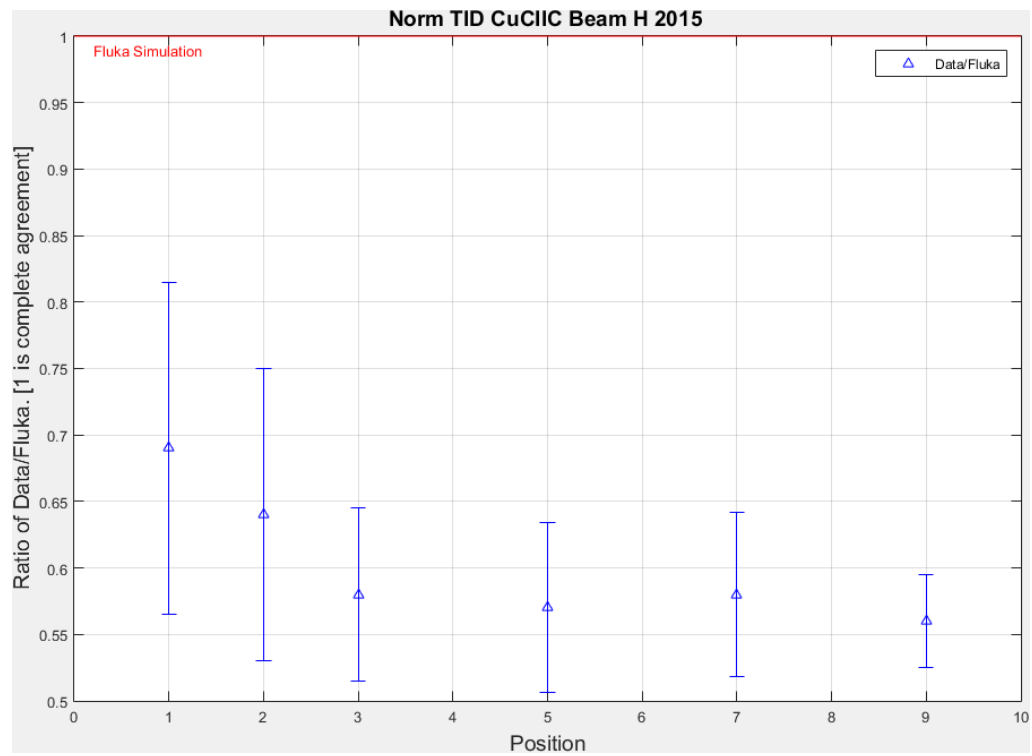


Figure 7-6: Agreement between V6 data and simulation on HEHeq for Cu\_CIIC

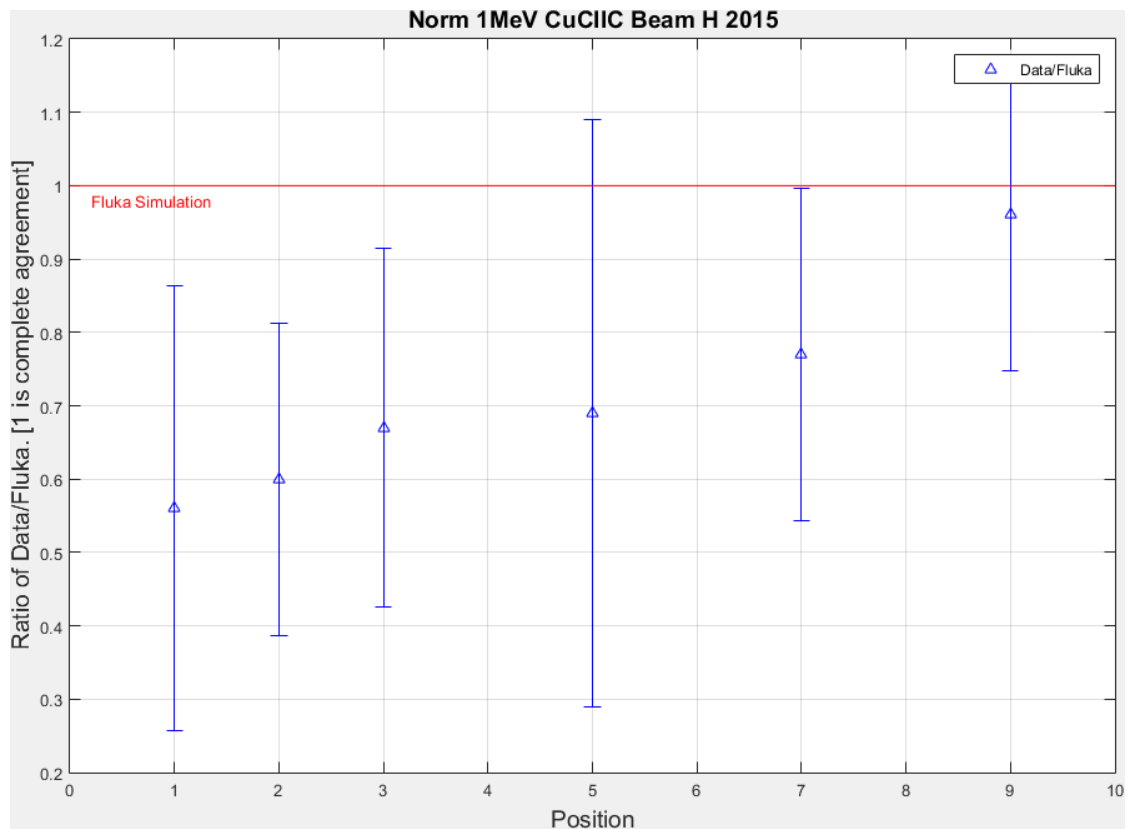


Figure 7-7: Agreement between 1-MeV neutron equivalent measurement and simulation for Cu\_CIIC. A data/FLUKA ratio of 0.56 to 0.96 strongly suggests a correlation with position on  $\Phi_{eq}$  fluence, with  $2.55E11 \Phi_{eq} \text{ cm}^2$ . This needs to be verified in simulation.

With a large R factor, position 1 was of interest to perform joint RadMON V5 and V6 HEH measurements. A gateway error prevented data recording for the V5, however it is foreseen to redo this measurement in 2015. Testing on this configuration prompted a neutron folding analysis [10]. Preliminary information on the intermediate neutron energy cross section of the Cypress lead a better accuracy of the HEHeq simulated value considering the intermediate neutron energy effects of the RadMON V6.

The large R factors observed in positions perpendicular to the target reveal the strong contribution from thermal neutrons with respect to the position closer to the beam line (where the field is dominated by high-energy charged hadrons). These values need still to be compared with new RadMON V5 measurements. The dose agreement is lower for this configuration. This is probably due to the fact that when using the shielding the particle field becomes even more dominated by the neutron component. As the FLUKA simulation is performed on a sensitive volume made of air (20cm\*20cm\*20cm), inside this sensitive volume the neutrons are depositing more energy than in a 100 nm silicon oxide. Therefore, this can induce a higher difference between simulation and measurements using the movable shielding inside the CHARM facility. In addition, the  $\Phi_{eq}$  measurements are in closer agreement to the simulation in positions of harder spectra.

## 7.4 Copper no shielding – Cu\_OOOO

Due to learned knowledge from the 2014 commissioning coupled with the higher RadMON V6 sensitivity and higher efficiency, three shorter Cu\_OOOO runs were performed which enabled collecting multiple measurements for each position.

Average of measurement when available for three Cu\_OOOO runs:

Run 1: 28/05/2015 20:06:00 to 29/05/2015 13:17:50 POT: 1.10E15

Run 2: 29/05/2015 20:25:00 to 30/05/2015 20:15:50 POT: 1.77E15

Run 3: 02/06/2015 09:59:00 to 02/06/2015 21:16:30 POT: 9.76E14

Position		Dose [Gy]	HEHeq cm <sup>-2</sup>	THEq cm <sup>-2</sup>	1-Mev NEQ cm <sup>-2</sup>	R Factor
1		Error %	Error %	Error %	Error %	
V6	Run 1	7.06E-15	2.48E-05	4.08E-05	2.74E-04	1.651
	MB7+DM7	6.4%	10.6%	8.7%	21%	
	Run 2	6.48E-15	2.48E-05 <sup>xviii</sup>	4.22E-05	2.88E-04	1.699
	MB7+DM7	11.7%	10.6%	8.7%	10.9%	
	Run 3	5.51E-15	3.13E-05	4.98E-05	1.80E-04	2.297
	MB6+DM6	5.6%	10.6%	8.7%	75%	
Average		6.35E-15	2.70E-05	4.43E-05	4.43E-05	
σ error of Samples		12%	14%	11%	11%	1.882
AvData / FLUKA		0.58	0.80		1.09	

Table 29: Measurements done on position 1 for CU\_OOOO configuration for V6 RadMONs

<sup>xviii</sup> This result is the same as in run 1

Position		Dose [Gy]	HEHeq cm <sup>-2</sup>	THeq cm <sup>-2</sup>	1-Mev NEQ cm <sup>-2</sup>	R Factor
1		Error %	Error %	Error %	Error %	
V5	Run 1	1.16E-14	2.46E-05	2.44E-05		1.070
		22.3%	10.6%	8.7%		
	Run 2	1.27E-14	2.54E-05	2.27E-05		0.893
		11.7%	10.6%	8.7%		
Average		1.22E-14	2.50E-05	2.36E-05		
σ error of Samples <sup>xix</sup>		6%	2%	5%	0.9811	
AvData / FLUKA		1.10	0.75			

Table 30: Measurements done on position 1 for CU\_OOOO configuration for V5 RadMONs

In addition to the difference in measured dose, thermal neutron fluence measured by the V5 is 50% of that measured by the V6. As intended in further testing, due to the gateway error, it is needed to collect more R factor measurements between the V5 and the V6 in all positions.

The measurement in run 3 with RadMON V6#6 introduces variability in the data set when directly comparing with runs 1 and 2. Since these results introduce a significant difference from those measured by RadMONV6#7, more measurements and analysis of other possible factors that could have influenced the run 3 result should be taken into account. However, having calculated the uncertainty on those repeated measurements, the difference observed between each measurements is comprised in the uncertainty calculation.

Unfortunately, both V5 RadMONs reached the end of their usability in the end of run 3. Seen on TIMBER as a sharp drop in the ADC reference voltage for both motherboards, the breakdown was related to taking excessive dose. The refurbished motherboards did not take above 60Gy in the whole commissioning period – this was unexpected as the refurbished motherboards stopped working before absorbing 80Gy, and only discovered later in data analysis.

<sup>xix</sup> Standard error of samples calculated using excel's STDEV.S function

		Dose [Gy]	HEHeq cm <sup>-2</sup>	THEq cm <sup>-2</sup>	1-Mev NEQ cm <sup>-2</sup>	R Factor
		Error %	Error %	Error %	Error %	
<b>Position 2</b>	Run 1	7.01E-15	2.25E-05	4.78E-05	2.41E-04	2.106
		13.4%	10.6%	8.7%	22%	
<b>V6 MB8 DM8</b>	Run 2	6.69E-15	2.35E-05	2.35E-05	2.70E-04	2.041
		11.1%	10.6%	8.7%	11.5%	
<b>V5</b>	Run 3	ADC breakdown during run				
<b>Average</b>		6.85E-15	2.30E-05	3.57E-05	2.56E-04	
<b>σ error of Samples</b>		3%	3%	48%	8%	2.07
<b>AvData / FLUKA</b>		0.57	0.66		0.98	
<b>Position 3</b>	Run 1	1.28E-14	3.87E-05	4.73E-05	2.42E-04	1.225
		10%	10.6%	8.7%	21.7%	
<b>V6 MB3 DM3</b>	Run 2	1.31E-14	3.94E-05	4.98E-05	2.67E-04	1.267
		9.7%	10.6%	8.7%	11%	
	Run 3	1.18E-14	4.26E-05	5.28E-05	1.82E-04	1.243
		7.9%	10.6%	8.7%	78%	
<b>Average</b>		1.26E-14	4.02E-05	5.00E-05	2.25E-04	
<b>σ error of Samples</b>		5%	5%	6%	19%	1.25
<b>AvData / FLUKA</b>		0.55	0.80		0.82	
<b>Position 5</b>	Run 1	9.43E-15	3.45E-05	4.41E-05	1.19E-04	1.220
	<b>MB4</b>	5.8%	10.6%	8.7%	44%	
<b>V6</b>	Run 2	9.76E-15	3.59E-05	4.22E-05	2.05E-04	1.231
	<b>MB4</b>	5.5%	10.6%	8.7%	19.7%	
	Run 3	8.60E-15	3.83E-05	4.44E-05	1.44E-04	1.159
	<b>MB5</b>	8.1%	10.6%	8.7%	16.6%	
<b>Average</b>		9.26E-15	3.62E-05	4.36E-05	1.56E-04	
<b>σ error of Samples</b>		6%	5%	3%	28%	1.20
<b>AvData / FLUKA</b>		0.44	0.95		0.72	

Table 31: Measurements performed on positions 2-5 in the Cu\_OOOO configuration



Variability is seen again in the thermal neutron fluence measurement on position 2, this time with the same V6 RadMON. This is not seen on position 3 with RadMON V6#3. A 10% difference is seen in the dose measurements between RadMONV6#4 and RadMONV6#5 on position 5 shows a good agreement between measurements.

		Dose [Gy]	HEHeq cm <sup>-2</sup>	THeq cm <sup>-2</sup>	1-Mev NEQ cm <sup>-2</sup>	R Factor
		Error %	Error %	Error %	Error %	
Position 9	Run 1	1.16E-14	3.59E-05	4.19E-05	1.63E-04	1.157
		12%	10.6%	8.7%	33.4%	
V6	Run 2	1.07E-14	3.71E-05	4.30E-05	1.87E-04	1.164
		8.6%	10.6%	8.7%	14.7%	
MB6 DM6	Run 3	1.10E-14	3.79E-05	4.67E-05	9.19E-05	1.235
		9.4%	10.6%	8.7%	17%	
Average		1.11E-14	3.70E-05	4.39E-05	1.87E-04	
STDev of Samples		4%	3%	6%	9%	1.19
AvData / FLUKA		0.54	0.89		1.09	

Table 32: Results from position 9 on CU\_OOOO with RadMON V6

		Dose [Gy]	HEHeq cm <sup>-2</sup>	THeq cm <sup>-2</sup>	1-Mev NEQ cm <sup>-2</sup>	R Factor
		Error %	Error %	Error %	Error %	
V5	Run 1	2.16E-14			3.01E-04	
		8.9%			22.7%	
DM5		1.91E-14			3.04E-04	
		8.8%			14.2%	
DM3	Run 2	2.14E-14			2.69E-04	
		5.2%			27.2%	
		2.13E-14			2.11E-04	
		5.9%			49.8%	
Average		2.14E-14			2.60E-04	
STDev of Samples						
		6%			11%	
AvData / FLUKA						
		1.04			1.52	

Table 33: Results from position 9 on CU\_OOOO with RadMON V5

For position 9 the same consistency in RadMON systems is revealed for different runs. However, the dose measurement of the V6 is 50% lower than the one of the V5 and the 1-MeV neutron equivalent fluence measured by the V5 is 50% higher than the V6 as it was also the case for position 9 using the AI\_OOOO configuration (see Table 26).

Further tests indicated that the dose measurement of the V5 could not be taken at face value. RadFETs, the CHARM BLM and optical fiber measurements all showed results 30-50% below simulation<sup>xx</sup>. This problem is however still under investigation; however, it is suspected that the refurbished V5 RadMONs were not working properly during these runs. A Co60 TID test between different V5 and V6 a good agreement between them with respect to the TID measurement performed with the 100 nm RadFET<sup>xxi</sup>. Therefore, either the RadMON V5 installed at CHARM do not work properly regarding TID measurement, or the radiation field at CHARM influence the measurement of both V5 and V6. This needs to be further investigated.

		Dose [Gy]	HEHeq cm <sup>-2</sup>	THEq cm <sup>-2</sup>	1-Mev cm <sup>-2</sup>	NEQ	R Factor
		Error %	Error %	Error %	Error %		
<b>Position 7</b>	Run 1	1.17E-14	3.68E-05	3.91E-05	1.71E-04		1.062
	<b>MB5</b>	14.3%	10.6%	8.7%	14%		
	Run 2	1.16E-14	3.84E-05	4.04E-05	1.98E-04		1.053
	<b>MB5</b>	8.8%	10.6%	8.7%	13.6%		
	Run 3	1.20E-14	4.23E-05	4.49E-05	1.89E-04		1.068
	<b>MB4</b>	6.2%	10.6%	8.7%	17.5%		
<b>Average</b>		1.18E-14	3.92E-05	4.15E-05	1.86E-04		
<b>STDev of Samples</b>		2%	7%	7%	7%		1.06
<b>AvData /FLUKA</b>		0.52	0.86		0.92		
<b>Position 10</b>	<b>V6</b>	1.36E-14	5.69E-05	4.05E-05	1.16E-04		
	<b>(DM7+DM7)</b>	9.7%	10.6%	8.7%	16.9%		0.717
	<b>Run 3 Data/FLUKA</b>	0.57	1.17		0.66		

Table 34: Results from position 7, single result from position 10 on Cu\_OOOO with RadMON V6

<sup>xx</sup> References pending at the time of writing.

<sup>xxi</sup> Reference pending

As it has already been mentioned for the other configurations and positions, all RadMON V6 TID measurements show a difference of around 40-50 % with FLUKA. This effect needs to be investigated in more details.

As seen in the two figures below, more results from position 10 are needed to be integrated with the data set. The ratio between data and simulation is rather large in this position. Since the measurement was performed with RadMONV6#7, although in the last run, it is not evident why this discrepancy was found.

A large ratio in the opposite sense is seen is found on the  $\Phi_{eq}$  reading. It can be observed in Fig 7.8, that there is also between 30% and 40 % difference between the measurement and simulation. It can be observed in Figure 7-10 that there is also between 30% and 40 % difference between the measurement and simulation. It is possible that the RadMON window did not face directly the target, and this is an important detail that must be taken into account for further measurement. It is possible that the direction of the RadMON window did not face the target, and this is an important detail that must be taken into account in further measurement. This attracts attention to further measurements in the first and last positions on the testing chamber.

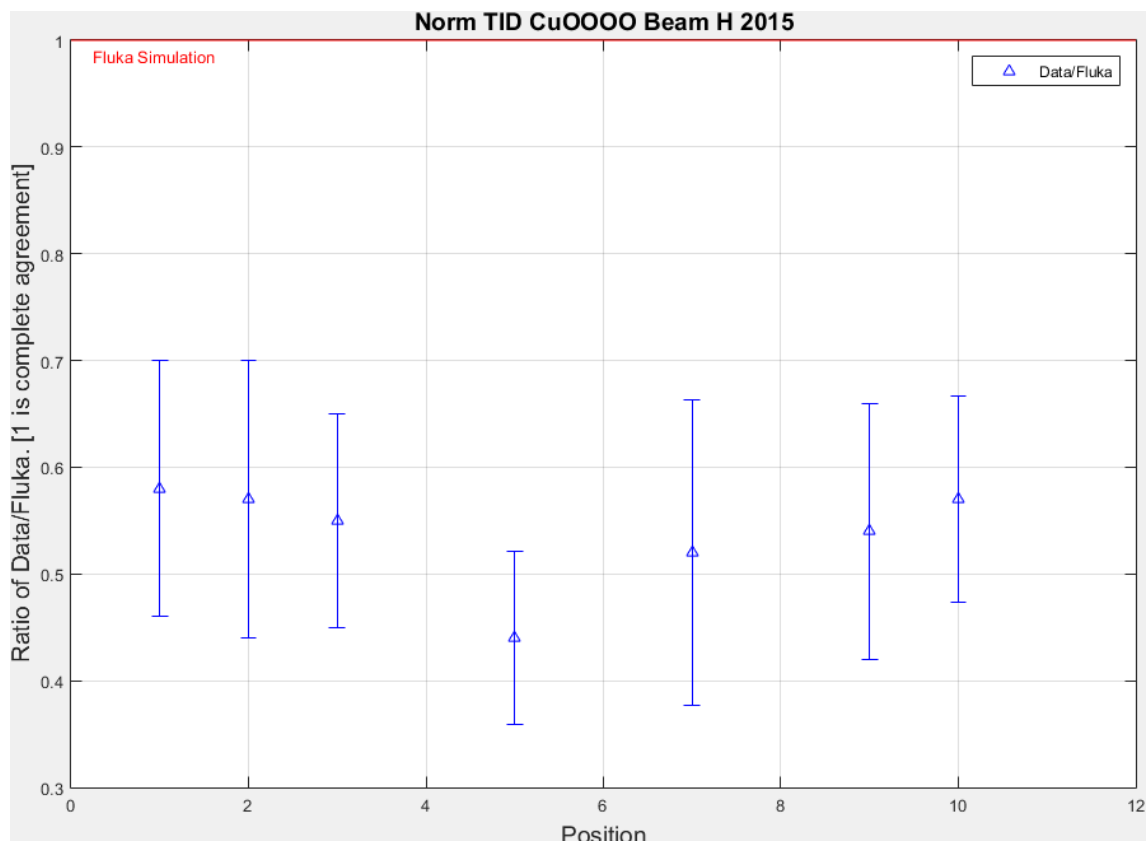


Figure 7-8: Agreement between V6 data and simulation on TID for Cu\_OOOO

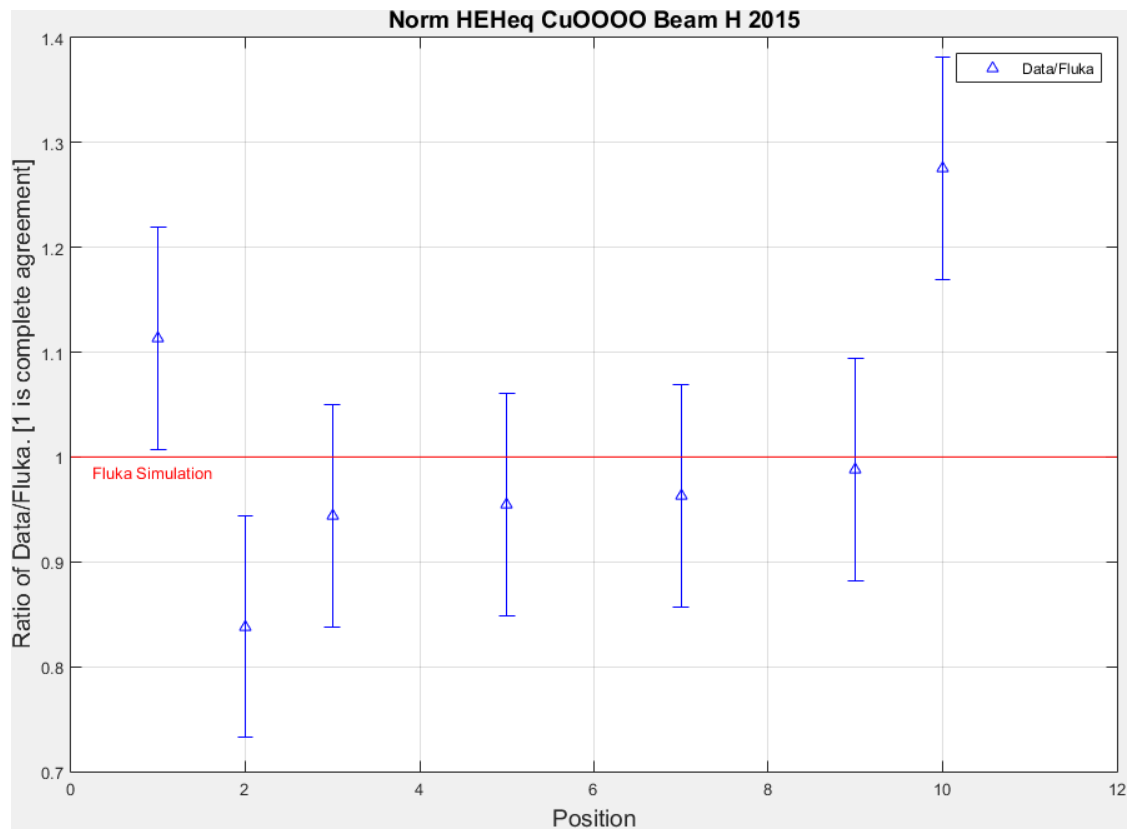


Figure 7-9: Agreement between V6 data and simulation on HEHeq for Cu\_OOOO

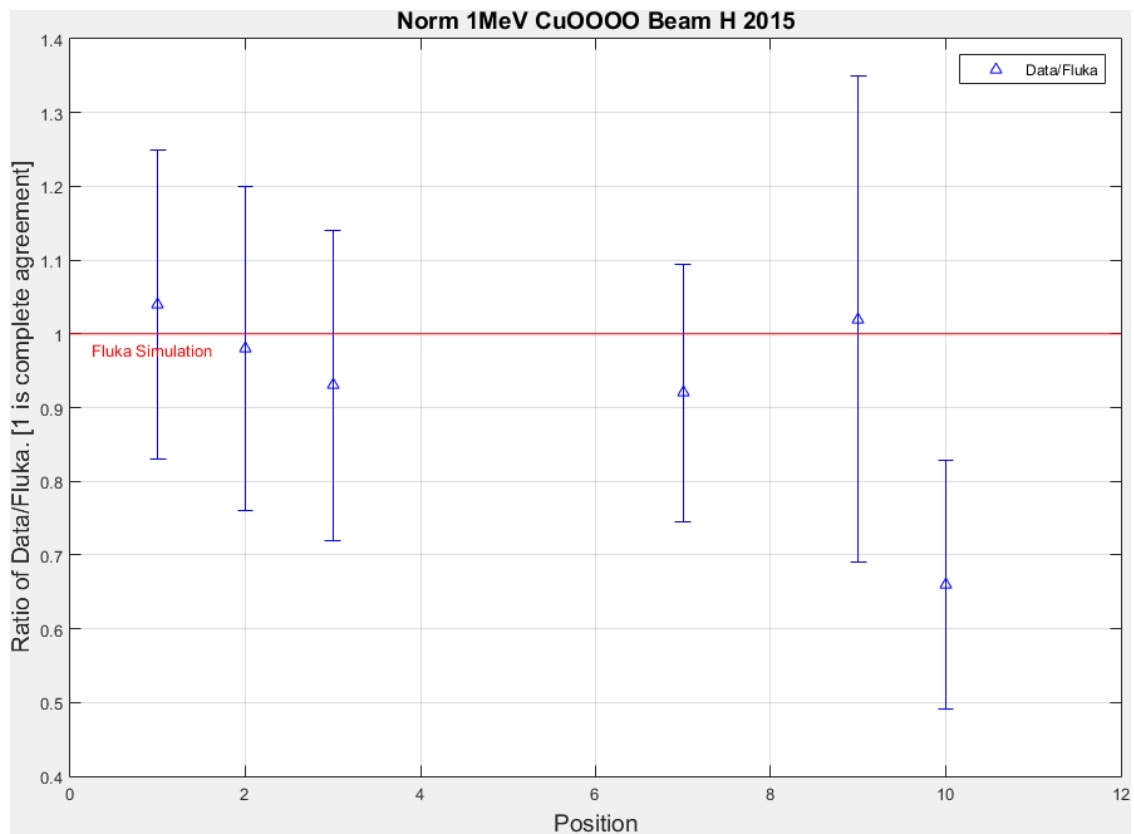


Figure 7-10: Agreement between V6 data and simulation on  $\Phi_{eq}$  for Cu\_OOOO

## 7.5 Measurements on the MONTRAC from 18.05.2015 to 29.06.2015

To complement 2014 measurements, the measurement type on the Montrac positron was expanded into  $\Phi_{eq}$  fluence measurement and a larger measurement area with RadFETs. The 27 RadFET card was always placed in front of the 15 3-PIN diode array.

Date <sup>xxii</sup>	RadMON/RadFETs	Beam type
22/05/2015	Radfet Card (x15)	Beam on Cu target (CIIC)
09/06/2015	RadFET (x27) and PIN diode card (x15)	Beam on Cu target
22/06/2015	DM V6#4 with 2 x 100nm RadFETs	Blown up beam
29/06/2015	RadFET (x27) and PIN diode card (x15)	Blown up beam

Table 35: Montrac irradiation run in the 2015 Commissioning period

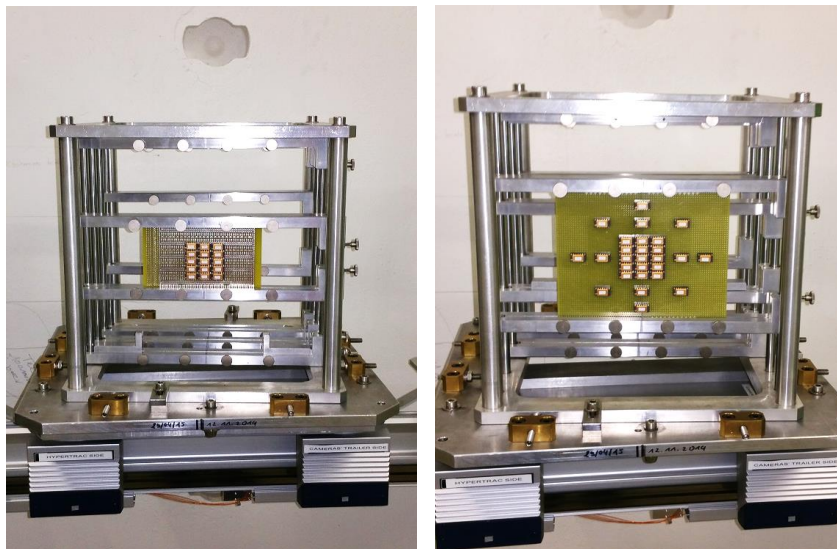


Figure 7-11 Both RadFET cards and mounted in the Montrac : Left: RadFET(x15) and Right: RadFET (x27)

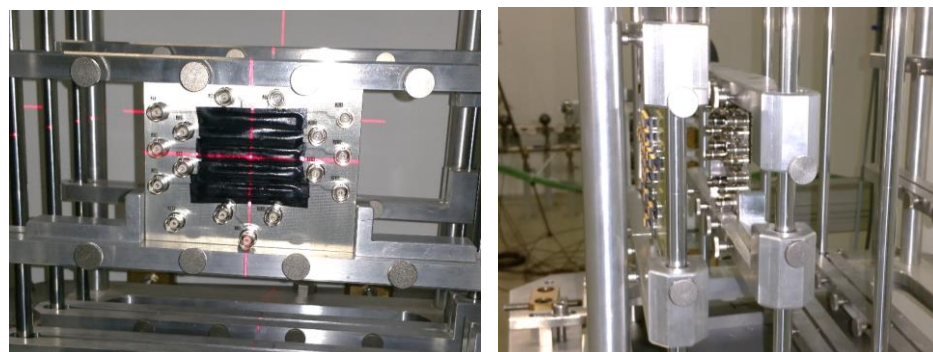


Figure 7-12 PIN diodes and RadFET cards installed on the Montrac. Profile view of both cards - note that the RadFET card was placed in front

<sup>xxii</sup> Detailed timing in tables 35 to 40

Montrac Radfet Board run during CU CIIC run 2015				Distance from center (mm)
Start: 22/05/2015 11:08:22	1.83E-13 0.77	2.69E-13 1.13	9.86E-14 0.41	20mm
End: 22/05/2015 18:08:48	2.31E-13 0.97	2.28E-13 0.96	1.59E-13 0.67	10mm
POT: 4.16E+14	3.22E-13 1.65	2.38E-13 1.00	5.29E-14 0.22	0
	2.69E-13 1.13	2.36E-13 0.99	2.14E-13 0.90	10mm
	2.02E-13 0.85	2.09E-13 0.88	1.71E-13 0.72	20mm
Distance from center (mm)	18 mm	0	18 mm	

Table 36: Dose measurements on the Montrac with a short circuit RadFET array

Next steps in this regard can include a correlation between the MWPC profile and the RadFET and PIN diodes maps measurements in order to use the MWPC to evaluate the dose and 1-MeV neutron eq. fluence profile at the Montrac test location.

Like in the previous chapter the ratio of result with RadFET in the center is presented below the dose calibration factor. The distances shown are from the center of the RadFET on the center to the RadFET on the grid. The sensitive volume of the RadFET is in the center of the RadFET.

Montrac Radfet Board run during CU OOOO run 2015								Distance to center
Start: 09/06/15 11:47:06 End: 11/06/15 06:05:00 POT: 4.16E+14	6.24E-14							60mm
	0.18							
	6.91E-14		8.26E-14		6.18E-14			40mm
	0.20		0.24		0.18			
	1.93E-13			1.95E-13	1.40E-13			20mm
	0.56			0.57	0.41			
	2.57E-13			2.74E-13	1.82E-13			10mm
	0.75			0.80	0.53			
	5.97E-14	1.06E-13	2.92E-13	3.43E-13	1.65E-13	1.27E-13	6.24E-14	0
	0.17	0.31	0.85	1.00	0.48	0.37	0.18	
								10mm
								20mm
								40mm
								60mm
Distance to center (mm)	74mm	46mm	18 mm	0	18 mm	46mm	74mm	

Table 37: Dose measurements on the Montrac with a short circuit RadFET array

From Table 37 and Table 18 for 2015 and 2014 measurements respectively, the dose measurements are in the same magnitude range. These are also in agreement with deployed module measurements in 2014 downstream from the copper target (Table 17)

Montrac PIN Diode Board run during CU 0000 run 2015				Distance from center (mm)
Start:	5.97E-04	6.00E-04	6.00E-04	
09/06/15	0.79	0.79	0.79	20mm
11:47:06	6.80E-04	7.63E-04	6.20E-04	
End:	0.90	1.01	0.82	10mm
11/06/15	7.54E-04	7.56E-04	6.97E-04	
06:05:00	1.00	1.00	0.92	0
POT:	7.40E-04	6.91E-04	6.28E-04	
4.16E+14	0.98	0.91	0.83	10mm
	6.94E-04	6.37E-04	4.94E-04	
	0.92	0.84	0.65	20mm
Distance from center (mm)	18 mm	0	18 mm	

Table 38: 1-MeV Neutron  $\Phi_{eq}$  measurements on the Montrac with a PIN diode array

Montrac PIN Diode Board run during Blown up Beam run 2015				Distance from center (mm)
Start:	4.64E-03	4.07E-03	3.79E-03	
29/06/15	0.93	0.82	0.76	20mm
20:49:07	3.95E-03	3.85E-03	3.26E-03	
End:	0.79	0.77	0.65	10mm
29/06/15	3.79E-03	4.99E-03	3.27E-03	
21:49:20	0.76	1.00	0.66	0
POT:	4.15E-03	3.33E-03	3.29E-03	
1.09E+14	0.83	0.67	0.66	10mm
	4.18E-03	3.82E-03	5.27E-03	
	0.84	0.77	1.06	20mm
Distance from center (mm)	18 mm	0	18 mm	

Table 39: 1-MeV Neutron  $\Phi_{eq}$  measurements on the Montrac with a PIN diode array



## Montrac Radfet Board run during Blown up Beam run 2015

								Distance to center
Start: 29/06/15 20:49:07  End: 29/06/15 21:49:20  POT: 1.09E+14								60mm
								40mm
								20mm
								10mm
	9.20E-14	8.10E-13	2.09E-12	2.32E-12	1.52E-12	2.95E-13	0.00	0
	0.04	0.35	0.90	1.00	0.66	0.13	0.00	
								10mm
								20mm
								40mm
								60mm
Distance to center (mm)	74mm	46mm	18 mm	0	18 mm	46mm	74mm	

Table 40: Dose measurements on the Montrac with a short circuit RadFET array

## 7.6 2015 Data summary tables with ratio of Data/FLUKA

### 2015 Commissioning period Cu\_OOOO configuration data (averages)

Position	TID Error Data/FLUKA	HEHeq CYP Error Data/FLUKA	Theq	1-Mev NEQ Error Data/FLUKA	R factor
<b>1 (V6)</b>	6.35E-15 12% 0.58	2.70E-05 11.9% 1.02	4.43E-05	2.47E-04 22% 0.94	1.33
<b>2 (V6)</b>	6.85E-15 13% 0.57	2.30E-05 10.9% 0.84	3.57E-05	2.56E-04 21% 0.98	2.07
<b>3 (V6)</b>	1.26E-14 10% 0.55	4.02E-05 11.2% 0.94	5.00E-05	2.25E-04 21% 0.82	1.25
<b>5 (V6)</b>	9.26E-15 8.1% 0.44	3.62E-05 11.2% 0.95	4.36E-05	1.56E-04 44% 0.72	1.20
<b>7 (V6)</b>	1.18E-14 14.3% 0.52	3.92E-05 10.8% 0.96	4.15E-05	1.86E-04 17.5% 0.92	1.06
<b>9 (V6)</b>	1.11E-04 12% 0.54	3.70E-05 12% 0.99	4.39E-05	1.87E-04 33.4% 1.09	1.19
<b>10 (V6)</b>	1.36E-14 9.7% 0.57	5.69E-05 10.6% 1.28	4.05E-05	1.16E-04 16.9% 0.66	0.72
<b>1 (V5)</b>	1.22E-14 22.3% 1.10 (400nm)	2.50E-05 12.7% 0.75	2.36E-05		0.98
<b>9 (V5)</b>	2.14E-14 8.9% 1.04			2.60E-04 49.8% 1.52	

Table 41 Summary of 2015 Cu OOOO results

## 2015 Commissioning period AI\_OOOO configuration data

Position	TID Error Data/FLUKA	HEHeq CYP Error Data/FLUKA	$T_{eq}$	1-Mev NEQ Error Data/FLUKA	R factor
<b>1 (V6)</b>	2.42E-15 11.9% 0.58	8.95E-06 10.6% 1.15	8.98E-06	5.42E-05 45% 0.98	1.01
<b>2 (V6)</b>	2.82E-15 16.5% 0.60	8.30E-06 10.7% 0.99	1.18E-05	6.20E-05 46% 1.08	1.38
<b>3 (V6)</b>	6.02E-15 6.3% 0.61	1.55E-05 10.7% 1.00	1.30E-05	5.45E-05 45% 0.78	0.83
<b>5 (V6)</b>	5.03E-15 18% 0.47	1.55E-05 10.7% 0.86	1.15E-05	5.54E-05 45% 0.85	0.74
<b>7 (V6)</b>	7.32E-15 7% 0.60	1.79E-05 10.7% 0.97	1.17E-05	6.24E-05 43% 0.96	0.64
<b>9 (V6)</b>	7.80E-15 17% 0.60	1.63E-05 10.7% 1.02	1.34E-05	6.73E-05 42% 1.08	0.69
<b>1 (V5)</b>	7.30E-15 10% 0.79 (400nm)	9.27E-06 12.7% 0.93	4.65E-06		0.52
<b>9 (V5)</b>	1.04E-14 17% 0.81 (#3 only)			1.06E-04 35% 1.71	

Table 42 Summary of 2015 AI OOOO results

### 2015 Commissioning period Cu\_CIIC configuration data

Position	TID Error Data/FLUKA	HEHeq CYP Error Data/FLUKA	Th <sub>eq</sub>	1-Mev NEQ Error Data/FLUKA	R factor
<b>1 (V6)</b>	4.67E-16 12.5% 0.69	1.34E-06 11.3% 0.86	2.73E-05	1.12E-05 30.3% 0.56	15.29
<b>2 (V6)</b>	4.82E-16 11% 0.64	1.51E-06 10.8% 0.74	3.03E-05	1.36E-05 21.3% 0.60	18.32
<b>3 (V6)</b>	7.60E-16 6.5% 0.58	2.74E-06 10.7% 0.69	2.01E-05	2.32E-05 24.5% 0.67	10.81
<b>5 (V6)</b>	1.00E-15 6.4% 0.57	2.94E-06 10.6% 0.72	2.79E-05	2.82E-05 40% 0.69	9.47
<b>7 (V6)</b>	1.18E-15 6.2% 0.58	3.45E-06 10.7% 0.76	2.92E-05	3.54E-05 22.7% 0.77	7.59
<b>9 (V6)</b>	1.53E-15 3.5% 0.56	4.36E-06 10.7% 0.85	2.81E-05	4.59E-0 21.3% 0.96	6.98

Table 43 Summary of 2015 CU CIIC results

## 7.7 2015 Commissioning period overview

The 2015 May-June commissioning period closed with a wealthy data set for three different configurations. The introduction of the RadMON V6, dedicated testing without user measurement constraints, standard position testing with repetitions and exchanges and careful run planning for the timespan of two weeks and two days are among the new factors at play in relation to 2014. New issues were raised as the difference in TID measurements between both RadMONs V5 and V6 were analysed with the same Matlab script and the same RadFET calibration table.

Recent results from alternate dosimetry equipment also puts data/FLUKA agreement at a ratio of 0.50-0.60. This sustains the case made by the V6 measurements and is currently one of the main priorities under analysis. High energy hadron and 1-MeV neutron-equivalent fluence measurements agree quite well with simulation, with the exception of the Cu\_CIIC configuration

In-beam measurements complete the data set in a high point with the first blown up beam measurements using short circuit RadFETs and PIN diodes where the TID

measurement is in line with previous data. Results from this commissioning period helped to set a clear set of goals for further measurement, to be discussed in chapter **Error! Reference source not found..**

## 8. REFERENCES

- [1] A. Thornton, "CHARM Facility Test Area Radiation Field," 2015 -.
- [2] E. J. Otedal, "CHARM SEC Report," Location: dfs/Projects/R2E/CHARM/Documentation/Final\_Documentation2015, 2015.
- [3] S. Danzeca, The new version of the Radiation Monitor system for the electronics at CERN. Electronics components radiation hardness assurance and sensor qualification., Geneva: University Montpellier 2, 2015.

## 9. 1. COMPARISON Between Measurements and Fluka simulations

Comparison made for 2014 results:

- During the 2014 campaign, RadMONs V5 have been used to calibrate the radiation levels inside CHARM.
- All the values to provide to the users (TID, HEH and  $\Phi_{eq}$  fluences) were given with a 50% uncertainty, thus being conservative and covering the maximum uncertainty reported on the difference between measurement and simulation.
- For TID comparison, it has to be mentioned that one factor which still need to be evaluated is the difference between simulated dose scored in air and in SiO<sub>2</sub>. Indeed, as using the RadFETs, the TID is measured in Gy(SiO<sub>2</sub>) and in Fluka the simulations are scored in air, a difference can occur. For this reason, new simulations are currently ran using the same geometry as the RadFET and the same material in order to evaluate the difference between TID(SiO<sub>2</sub>) and TID(air). .

[\[JM1\]](#) Results provided during the 2015 campaign completed the 2014 ones. During this period, six RadMON V6 were used in addition with two RadMON V5. The latter being used for comparison purpose with the RadMON V6.

For TID measurement, a difference between the V6 measurements and Fluka simulation between 30 and 50 % can be observed. On contrary, other experimental measurement made using short circuited RadFETs (located close to the optical fibers), optical fiber, RPL and BLM, show also a difference in the order of 40-50 %, therefore confirming what is measured by the V6. However, the measurements made with the RadMON V5 show a lower difference with Fluka, and therefore a 20-40% difference with the V6 measurement.

It has to be mentionned, that a comparison between RadMON V5 and V6 measurement has been performed at the Co-60 facility[\[JM2\]](#) , showing identical RadFET radiation response using both system.

The RadMON V5 have been changed in July 2015 to investigate if this difference was due to the RadMON used at CHARM. Even by changing the RadMON V5, up to now this difference is still observed. An investigation is currently being performed to understand where this difference is coming from.

For configurations without shielding, the agreement is very positive regarding the HEH and  $\Phi_{eq}$ fluence.

The resolutions from 2014 concerning Cu\_OOOO have evolved with repeat measurements in 2015:

- Total ionising dose is still to be taken at face value, favouring the V6  $\pm$  30% error
- Simulated HEHeq fluence is in good agreement with data –its results are accepted for CHARM usage  $\pm$  50% error (to be decided)
- Simulated 1-MeV N.E. fluence is also in good agreement with data and the simulation can be relied upon for CHARM usage on this aspect of the mixed radiation field  $\pm$  50% error (to be decided)

Future FLUKA research will offer new comparison points with in-beam testing results and possibly shed new light on the current TID measurement challenge and possible correlation between radiation field flux and agreement with measurement.

## 10. 2. FUTURE MEASUREMENTS, RECOMMENDATIONS

### 10.1 2.1 Completing the FLUKA – RadMON comparison

Two challenges to a definitive first complete benchmark with FLUKA are:

- Difference between the TID measurements made with the V5 and the V6.

Current pertinent information:

- V5 motherboards at CHARM are refurbished from 2014 and broke down before reaching 60 Gy instead of 80 Gy [\[JM3\]](#)
- V6 RadMONs were new and more robust to radiation
- Measurement with short circuited RadFETs following radio-photoluminescence dosimeters (RPL's) in custom positions near the walls behind position 1 , around the target and on position 13 show simulation to be 1.8 to 3 times as large as measurement (Performed during Cu\_CIIC and Cu\_OOOO run 3 2015)
- Recent information from BLM data analysis shows a rough 50% agreement (0.50) with FLUKA simulation [\[JM4\]](#)

Steps being taken to achieve a definitive TID data measurement to compare with FLUKA:

- V5/V6 measurement with new RadMONs in C60 facility, revealing good agreement between 100nm measurements (nevertheless only the deported modules have been irradiated)

Figure 9-1: Dose measurement by V5 and V6 on a 5Gy/hr C60 facility

- Independent cross check of results
- Measurements done with user irradiation using a new V5 RadMON on positions 2 and 10 using deported modules being analysed at the time of writing
- Planning of further V5 and V6 joint measurements in the CHARM mixed field
- Finalisation of the SEC factor calibration as it has been seen that there is a 20%-30% difference between the calibration done using the fast beam extraction and the measurement performed with the Aluminium foils. [\[JM5\]](#)
- SEC 1 calibration factor

#### Current pertinent information:

- IRRAD work has made it necessary to rely on SEC1 for POT tracking as it has been demonstrated in section ...
- SEC1 and SEC2 are linear after  $1E11$  protons per spill
- SEC1 calibration factor has changed from  $1.99E7$  protons per count (in 2014) to  $2.24E7$  (in 2015) as a compromise between aluminium irradiation foil measurements and fast beam current transformer (FBCT) results relatively –
- A paper by V.Agoristas from 1968 [8] advises briefly on page 21 to count on a 20% efficiency loss of SEC measurement on fast current transformer reading (no references or data) – SEC's are few and usually custom built thus there is little literature on the subject. An email response from the responsible of their installation, J. Spanggaard expresses unfamiliarity with this result and casts doubt over the feasibility of using SEC's with FBCT calibration.
- The cross section of Aluminium at 24 GeV/c protons is an approximation from 20 GeV protons from (ref paper [\[JM6\]](#) ) using historical references
- There is a combined 7% error in HPGe gamma detector calculation when measuring the activity of aluminium foil samples. It is checked regularly using a multi-gamma source (checked independently from RP procedure).
- All factors considered, the 20% lower Al foil measurement factor combined with the nota bene of V.Agoristas are currently construed as more than coincidence in determining the SEC1 count to proton calibration factor [\[JM7\]](#)
- For the time being and in this report a calibration factor of  $2.24E7$  is used. A lowering in this factor would bring a closer agreement with TID measurements and simulation, but a larger difference with the HEH fluence.

Steps being taken to achieve a definitive SEC calibration factor and thus an accurate POT value:

- Verifying current data with parties involved

- Further 24 GeV proton flux tests by measuring the radioactivity of irradiated foils of other materials (probably not possible since the cross-section of other materials at such energy (e.g. for Copper foils) is not well known.)
- ESA SEU monitor measurements and analysis to be completed.
- Researching other methods to probe beam intensity and analysing dosimetry of in-beam measurements

## 10.2 2.2 Building on current RadMON data set

It is desirable to push the envelope on current knowledge of the mixed field on locations that are challenging to simulate. Recommended testing goals with the RadMON include:

- Completing AI and AIH data set with repeat measurements with and without shielding, partial shielding data sets for all targets
- Testing positions 11-13 on harder spectra, R factor measurements on short runs if possible. In this case we have to keep in mind that the gradient at such positions is very important.
- R factor measurements using the V5 and V6 on positions 1-3 and as much as possible on Cu\_CIIC
- Verifying field gradient at different heights for different positions and configurations (simulation predicts variability with positions)[\[JM8\]](#)
- Passive dosimetry on walls and testing chamber entrance
- Analysis of SEU's on motherboards stored in the rack during runs (visible and possible to analyse)
- Further co-ordinated passive/online RadMON/optical fiber measurements
- Identifying and correcting Cypress bursts – The algorithm to remove the burst into the Cypress is currently being tested at CHARM
- In-beam testing downstream from aluminium targets and in-beam HEH fluence measurements
- Additional radiation hardness and spectra measurements with appropriate detectors

Potential future improvements

- Strict positioning procedure of RadMON in commissioning period measurements (i.e.: the casing window of all RadMON's must face the target, not a wall)
- Wireless positioning recording system for RadMONs and user devices.

Future error analysis work should explore:

- RadMON to RadMON variation of systems installed at CHARM
  - SRAMs, RadFET, PIN diode measurements

## 10.3 2.3 Working with IRRAD to understand influence on the CHARM mixed radiation field downstream and managing CHARM response accordingly

It was found that IRRAD sample influence had a negligible effect on the data measurements of 2014, but this is not guaranteed in the future.



New measurements are currently demonstrating that dense samples installed into IRRAD (e.g. Crystal) can lead to a strong degradation of the dose rate and the flux of the primary proton beam, inducing a decrease of the dose rate and fluxes of the mixed field.

As IRRAD is upstream from CHARM it is clear that there must be communication between both facilities and that CHARM personnel is informed when IRRAD introduces samples of considerable density into the beam.

There should be a decision of whether data collected at CHARM is discarded or used with adjustments based on very little information on interactions upstream from the target.

It is also recommended to perform a joint test with IRRAD supported by simulation where samples of increasing density and stopping power for 24GeV protons are introduced into the beam in order to find a threshold past which the mixed radiation field at CHARM would be affected beyond doubt.

An agreement then could be made on these grounds that IRRAD should not insert samples with a stopping power exceeding this limit without informing CHARM and an evaluation made whether CHARM performance would be acceptable under such conditions for irradiation and benchmarking purposes.

## 11. 3. REFERENCES

[1]	A. Thornton, "CHARM Facility Test Area Radiation Field," 2015 -.
[2]	E. J. Otedal, "CHARM SEC Report," Location: dfs/Projects/R2E/CHARM/Documentation/Final_Documentation2015, 2015.
[3]	S. Danzeca, The new version of the Radiation Monitor system for the electronics at CERN. Electronics components radiation hardness assurance and sensor qualification., Geneva: University Montpellier 2, 2015.

[JM9]

## 12. 4. Appendixes

### 12.1 4.1 Online data files

Every source file for every result with plots for every k factor will be saved on the dfs and also put online.

Description	URL
Charm Run Log	<a href="http://cern.ch/go/F9nZ">http://cern.ch/go/F9nZ</a>
RadMON Locations 2014	<a href="http://cern.ch/go/Jsr9">http://cern.ch/go/Jsr9</a>
RadMON Locations 2015	
Automatic FLUKA Reporting	<a href="http://cern.ch/go/C6bk">http://cern.ch/go/C6bk</a>
Average Data Results	<a href="http://cern.ch/go/7LNT">http://cern.ch/go/7LNT</a>

<b>Scripts and original data 2014</b>	
<b>Scripts and original data 2015</b>	

Table 40: Online file repository. This can change in the future.

## 12.2 4.2 Extrapolation of nuclear interaction range of Silicon for 24 GeV/c protons [\[JM10\]](#)

It is no longer necessary to input initial RadFET values by hand as these are stored in a matrix which is initially loaded but it is imperative that these are updated with every RadFET change in the CHARM RadMONs. Matrixes with the data must have the same size for algebra in Matlab.

All the results in this table show measurements in different positions for the CU\_OOOO configuration. The different times at which they were performed are indicated and the run of 12.11 provides most of the data. This run and the repeated measurements of Position 4 and Position 15 provided the basis for FLUKA-RadMON TID benchmarking in 2014.  $\Phi_{eq}$  data processing was completed in 2015. The issue is addressed further in the 2015 data set with repeat measurements for Cu\_OOOO. However unlike the 2015 V5 data set, the measured data is lower than simulated which however is in line with the average case for dose and HEH fluence.

As seen in the following chapter, TID measurements with the V5 were significantly larger than the V6, by 40-50%. This was confirmed with multiple dosimetry measurements from a variety of devices in 2015. A second look at the 2015 data set revealed an enlarged 1-MeV n.e.f. for the V5, whilst the V6 measurements were within 10-20% of simulation. This is seen again in retrospect for the case of 2014. Quite a few measurements were not performed at beam height. This is indicated accordingly for those which are shown, where these were taken close to beam height. Other results at non-standard heights were not included to keep in line with officially simulated FLUKA output.

There is a pattern of lower HEH response with respect to radiation hardness, properties of the field at closed (harder, more energetic spectra) and open angles (higher number of thermal neutrons, lower energy particles) to the target. [\[JM11\]](#)

[\[JM1\]](#) This does not mean anything !

[\[JM2\]](#) Please give a reference to raffaello and salvatore.

[\[JM3\]](#) When ? In 2014 or in 2015 ?

[\[JM4\]](#) Do you have a reference for this? Ask Maris (she's at CERN now)

[\[JM5\]](#) Reference to be added.

[\[JM6\]](#) To be asked to Markus

[\[JM7\]](#) What do you mean? Do you mean that on all the results you presented in this report, you consider the 20 % discrepancy for the SEC calibration factor ?

[\[JM8\]](#) Here you have to mention that this you did not put the value at different height that you have measured in 2014 – 2015. Please indicate where we can find those data.

[\[JM9\]](#) List of references to be completed

[\[JM10\]](#) What is this ?

[\[JM11\]](#) What is this ?

